

## Proper orthogonal decomposition in wind engineering. Part 2: Theoretical aspects and some applications

Luigi Carassale<sup>†</sup>, Giovanni Solari<sup>‡</sup> and Federica Tubino<sup>‡†</sup>

*DISEG, Department of Structural and Geotechnical Engineering,  
University of Genoa, Via Montallegro, 1, 16145 Genoa, Italy*

*(Received June 27, 2006, Accepted March 19, 2007)*

**Abstract.** Few mathematical methods attracted theoretical and applied researches, both in the scientific and humanist fields, as the Proper Orthogonal Decomposition (POD) made throughout the last century. However, most of these fields often developed POD in autonomous ways and with different names, discovering more and more times what other scholars already knew in different sectors. This situation originated a broad band of methods and applications, whose collation requires working out a comprehensive viewpoint on the representation problem for random quantities. Based on these premises, this paper provides and discusses the theoretical foundations of POD in a homogeneous framework, emphasising the link between its general position and formulation and its prevalent use in wind engineering. Referring to this framework, some applications recently developed at the University of Genoa are shown and revised. General remarks and some prospects are finally drawn.

**Keywords:** aerodynamics; digital simulation; proper orthogonal decomposition; random processes; turbulence; wind engineering.

---

### 1. Introduction

This paper is the logical prosecution of a companion paper (Solari, *et al.* 2007) that provides a state-of-the-art on the birth, the evolution and the most recent developments of the Proper Orthogonal Decomposition (POD), with special regard to its applications in wind engineering. That paper points out the plurality of the contexts where POD is applied, and the peculiarity that different fields often developed this technique in autonomous forms, discovering several times what other fields already knew, coining a long series of names and acronyms which certainly did not facilitate the homogeneity of this matter. This situation originated a broad band of fragmentary and variegated methods and applications, whose collation requires working out a comprehensive viewpoint on the representation problem for random quantities.

Right in this spirit, this paper illustrates some theoretical aspects of POD in a homogeneous and comprehensive framework (Section 2), stressing the different properties that characterise finite

---

<sup>†</sup> Assistant Professor

<sup>‡</sup> Professor, Corresponding Author, E-mail: [solari@diseg.unige.it](mailto:solari@diseg.unige.it)

<sup>‡†</sup> Post Doc Researcher

energy and infinite energy processes, and the link between the general position and the formulation of POD and its prevalent use in wind engineering. Some applications recently developed at the University of Genoa are also revised and embedded within this framework (Section 3). General remarks and some conclusions are drawn in Section 4.

## 2. Theoretical aspects

A zero-mean random process is fully represented, at the second order, by its covariance function. Unfortunately, the interpretation of physical phenomena via the study of such a quantity is often a difficult task since it is seldom supported by intuition. Under this viewpoint, it seems more appropriate representing a random process using quantities related to the shape of its typical realisations.

POD tries to achieve this purpose searching for deterministic shapes, the POD modes, which are representative, in some statistical sense, of the realisations of the process and can be used as functional-bases well suited for the construction of representation formulae. This method assumes different expressions whether or not the process can be idealised as stationary or homogeneous. Stationarity hypothesis is usually accepted for the representation of physical phenomena characterised by a time scale much faster than the observation period; the term homogeneous identifies the same property, but is usually referred to space. In the following treatment, a random process fulfilling the above property is generically referred to as stationary, except for the cases explicitly dealing with spatial coordinates for which the term homogeneous is adopted.

The representation problem is formalised in rather wide terms in Section 2.1, referring to random processes whose realisations are members of a generic inner-product vector space. The treatment is particularised first to random vectors with values in  $\mathbb{C}^n$ , attaining the formulation of the Principal Component Analysis (PCA) (Section 2.2). Section 2.3 extends the formulation to the case of finite-energy random processes leading to the Karhunen-Loeve Expansion (KLE). Section 2.4 provides a generalisation of these concepts to develop the representation of infinite-energy random processes, in particular stationary ones. An  $m$ -dimensional ( $m$ -D) process considered as stationary with respect to some dimensions and non-stationary with respect to the other ones is referred to as an incompletely stationary process and is treated in Section 2.5. In practical applications, the spatial coordinates are often discretised, leading to approximate an  $m$ -D process function of time and space with an  $n$ -variate ( $n$ -V) process function of time only; for such a process (whose realisations are trajectories in  $\mathbb{C}^n$ ) POD can be interpreted as a linear transformation whose properties are described in Section 2.6. Section 2.7 illustrates the use of POD-based representations for developing digital simulation procedures aimed at the generation of stationary and non-stationary Gaussian time series; the non-Gaussian case is briefly discussed for the sake of completeness.

### 2.1. Position of the problem

Let  $v$  be a zero-mean random vector whose realisations are in the vector space  $\mathcal{V}$ . Let us consider the problem of finding a deterministic vector  $\phi \in \mathcal{V}$  that represents the most typical realization of  $v$ , i.e., that maximises the likelihood measure:

$$J = E[|(v, \phi)|^2] \quad (1)$$

under the constrain:

$$\|\phi\|^2 = 1 \quad (2)$$

where  $E[\bullet]$  is the statistic average operator and  $(\bullet, \bullet)$  represents the inner product in  $\mathcal{V}$ ,  $\|\bullet\|$  being the corresponding norm. The problem represented by Eqs. (1) and (2) can be solved by maximising the functional:

$$J_1 = E[|(v, \phi)|^2] - \lambda \|\phi\|^2 = (C_v, \phi \otimes \phi) - \lambda \|\phi\|^2 \quad (3)$$

where  $\lambda$  is a Lagrange multiplier,  $C_v = E[v \otimes v]$  is the correlation (and also the covariance since  $v$  is zero-mean) of  $v$ , and  $\otimes$  represents the outer product in  $\mathcal{V}$ .

## 2.2. Representation of random vectors in $\mathbb{C}^n$

Let us consider the case in which  $\mathcal{V} \equiv \mathbb{C}^n$ , thus  $v$  is an  $n$ -V random vector whose realisations are in  $\mathbb{C}^n$ . In such a case, inner and outer products are particularised as:

$$(v, \phi) = \mathbf{v}^* \phi; \quad v \otimes \phi = \mathbf{v} \phi^* \quad (4)$$

where  $\mathbf{v}$  and  $\phi$  list the components of  $v$  and  $\phi$  along some base in  $\mathbb{C}^n$ , and the superscript  $*$  represents the conjugate transpose. Substituting Eq. (4) into Eq. (3), the functional  $J_1$  results:

$$J_1 = \phi^* C_v \phi - \lambda \phi^* \phi \quad (5)$$

where  $C_v = E[\mathbf{v} \mathbf{v}^*]$  is the covariance matrix of  $\mathbf{v}$ . The stationarity condition on  $J_1$  produces the equation:

$$C_v \phi = \lambda \phi \quad (6)$$

whose solutions  $\lambda$  and  $\phi$  are, respectively, the eigenvalues and the eigenvectors of the matrix  $C_v$ .  $C_v$  is (Hermitian) symmetric and non-negative definite, thus the eigensolutions of Eq. (6) are in number of  $n$ , the eigenvalues are real and non-negative, the eigenvectors are orthogonal (or can be chosen as orthogonal in case of multi-dimensional eigenspaces) and are considered here as orthonormal, i.e.,  $\|\phi_k\| = 1$ ,  $k = 1, \dots, n$ . From a geometrical point of view, the eigenvectors  $\phi_k$  ( $k = 1, \dots, n$ ) are the principal axes of the tensor  $C_v$ .

Any realisation of the vector  $\mathbf{v}$  can be represented as a linear combination of the eigenvectors through the formula:

$$\mathbf{v} = \sum_{k=1}^n \phi_k x_k \quad (7)$$

where  $x_k$  ( $k = 1, \dots, n$ ) are random variables referred to as the Principal Components (PC) of  $\mathbf{v}$ . Thanks to the orthonormality of the eigenvectors, such random variables result:

$$x_k = \phi_k^* \mathbf{v} \quad (k = 1, \dots, n) \quad (8)$$

Moreover, again for the orthonormality of the eigenvectors and for Eq. (6), it is easy to demonstrate that the PC are uncorrelated with each other and their variance is given by the corresponding eigenvalue:

$$E[x_h x_k^*] = \begin{cases} \lambda_h & \text{if } h = k \\ 0 & \text{otherwise} \end{cases} \quad (9)$$

If the eigenvalues are sorted in decreasing order, the first eigenvector  $\phi_1$  represents the typical (the most recurrent) direction of the random vector  $\mathbf{v}$ , while the first term of the sum in Eq. (7),  $\mathbf{v}^{(1)} = \phi_1 x_1$ , represents its best mono-variate approximation. The other terms,  $\mathbf{v}^{(k)} = \phi_k x_k$  ( $k=2, \dots, n$ ) contain components of  $\mathbf{v}$  that cannot be accommodated in  $\mathbf{v}^{(1)}$  and can be idealised as corrections of progressively decreasing amplitude.

The vector  $\mathbf{v}$  has been assumed as zero-mean; however, a non-zero mean value can be easily included in Eq. (7) as a deterministic addendum. In this way, the terms  $\mathbf{v}^{(k)}$  characterise the random fluctuation of  $\mathbf{v}$  around its mean value. Some authors, on the contrary, defined Eq. (6) using the correlation matrix, instead of the covariance matrix, obtaining eigenvalues and eigenvectors depending on the mean value of  $\mathbf{v}$ . In this case it happens that, if the mean value of  $\mathbf{v}$  is large with respect to its random fluctuation, the first eigenvector  $\phi_1$  tends to assume its direction, while the subsequent eigenvectors tend to characterise the random fluctuation orthogonal to the mean value.

Combining Eqs. (7) and (9) the covariance matrix  $\mathbf{C}_v$  can be expressed by the spectral decomposition (Mercer 1909):

$$\mathbf{C}_v = \sum_{k=1}^n \phi_k \phi_k^* \lambda_k \quad (10)$$

Eqs. (6)-(10) define a conceptual scheme for the representation of random vectors referred to as Principal Component Analysis (PCA).

### 2.3. Representation of finite-energy random processes

Let us consider the space  $\mathcal{V}$  of the complex-valued functions defined on the interval  $[a, b] \subset \mathbb{R}$ . Eqs. (1)-(3) can be particularised to the present case defining inner and outer products as:

$$(v, \phi) = \int_a^b v^*(t) \phi(t) dt; \quad v \otimes \phi = v(t_1) \phi^*(t_2) \quad (11)$$

which imply the necessity of restricting the space  $\mathcal{V}$  to square-integrable functions on  $[a, b]$ . This corresponds, from a physical point of view, to the assumption that the process  $v(t)$  has finite energy. It is possible to demonstrate through variational methods (Lumley 1970) that the functional  $J_1$  is stationary if  $\phi(t)$  and  $\lambda$  fulfil the condition represented by the integral Fredholm-type equation:

$$\int_a^b C_v(t_1, t_2) \phi(t_2) dt_2 = \lambda \phi(t_1) \quad (12)$$

where  $C_v(t_1, t_2) = E[v(t_1)v^*(t_2)]$  is the covariance function of the process  $v(t)$ ; the solutions  $\lambda$  and  $\phi(t)$  of Eq. (12) form an infinite denumerable set (i.e., its elements can be put in one-to-one correspondence with the set of the natural numbers  $\mathbb{N}$ ) and are, respectively, the eigenvalues and the eigenfunctions of  $C_v(t_1, t_2)$ .  $C_v(t_1, t_2)$  is (Hermitian) symmetric and non-negative definite, thus the eigenvalues are real and non-negative; the eigenfunctions are orthogonal with respect to the inner product defined by Eq. (11), and are considered here as orthonormal, i.e.,  $\|\phi_k(t)\| = 1$ ,  $k \in \mathbb{N}$ .

The analogy between Eq. (12) and Eq. (6) is quite evident; the substantial consequence of the passage to an infinite-dimensional space is the presence of an infinite number of eigensolutions. Likewise in the finite-dimensional case, however, such eigenfunctions constitute a base for the space

$\mathcal{V}$ , thus any realisation of the process  $v(t)$  can be expressed by the series expansion:

$$v(t) = \sum_{k=1}^{\infty} \phi_k(t)x_k \quad (13)$$

where  $x_k$  are random coefficients given by the projection of  $v(t)$  on the eigenfunctions:

$$x_k = \int_a^b \phi_k^*(t)v(t)dt \quad (k=1,2,\dots) \quad (14)$$

and are uncorrelated according to Eq. (9). Eqs. (13) and (14) are the obvious transposition of Eqs. (7) and (8) to the continuous case and, combined with the definition of the covariance function, provide a spectral representation formula analogous to Eq. (10):

$$C_v(t_1, t_2) = \sum_{k=1}^{\infty} \phi_k(t_1)\phi_k^*(t_2)\lambda_k \quad (15)$$

Eq. (13) is referred to as the Karhunen-Loeve Expansion (KLE) or the Proper Orthogonal Decomposition (POD) of the process  $v(t)$ , the eigenfunctions  $\phi_k(t)$  are referred to as POD modes, and the random coefficients  $x_k$  are defined as PC.

Eqs. (12)-(15) can be easily generalised to consider the case of  $n$ -V,  $m$ -D processes whose realisations have values in  $\mathbb{C}^n$  and are square-integrable functions over the domain  $\mathcal{D} \subset \mathbb{R}^m$  updating the definitions of the products given in Eq. (11).

#### 2.4. Representation of infinite-energy processes - Stationary random processes

As it has already been observed, the problem of the representation of infinite-energy processes cannot be studied following the above treatment. The realisations of such processes, indeed, are not likely to be square-integrable, thus the inner product in Eq. (11) cannot be defined. A technical consequence of this situation is that the convergence of the integral in Eq. (12), defining the POD modes, is not assured.

A relevant class of infinite-energy processes comprehends the stationary ones, whose realisations are not square-integrable since (almost surely) they do not vanish for  $t$  tending to infinite. Such kind of processes have the property that the covariance function  $C_v(t_1, t_2)$  does not depend on the parameters  $t_1$  and  $t_2$  separately, but only on their difference,  $\tau=t_1-t_2$ , i.e.;

$$C_v(t+\tau, t) = E[v(t+\tau)v^*(t)] = \tilde{C}_v(\tau) \quad \forall t \in \mathbb{R} \quad (16)$$

The symbol  $\sim$ , used to distinguish  $C_v$  (function of two variables) and  $\tilde{C}_v$  (function of one variable), is dropped in the following, whenever the choice between the two functions is clear from the context.

In the class of stationary processes, a relevant case in which the mentioned mathematical difficulties can be easily circumvented does exist and regards the so called mean-square-periodic processes. For such processes the following relationship holds (Papoulis 1965):

$$E[(v(t) - v(t+T))^2] = 0 \quad (17)$$

for some  $T$  representing the period. In this case, the maximisation of the functional  $J_1$  can be

performed on the finite interval  $[-T/2, T/2]$ , being assured to meet the likelihood requirement everywhere. If the realisations of  $v(t)$  are square-integrable over such an interval, Eqs. (11)-(15) perfectly hold just letting  $a=-T/2$  and  $b=T/2$ .

Eq. (17) implies that the covariance function  $\tilde{C}_v$  is periodic with period  $T$  (Papoulis 1965) and, as such, can be represented by the Fourier series expansion:

$$C_v(t_1, t_2) = \tilde{C}_v(t_1 - t_2) = \sum_{k=-\infty}^{\infty} e^{i\omega_k(t_1 - t_2)} s_k \quad (18)$$

where  $\omega_k = 2\pi k/T$  and  $s_k$  are the Fourier coefficients defined as:

$$s_k = \frac{1}{T} \int_{-T/2}^{T/2} e^{-i\omega_k \tau} C_v(\tau) d\tau \quad (19)$$

Substituting Eq. (18) into Eq. (12), it can be demonstrated that the eigensolutions  $\lambda$  and  $\phi(t)$  must have the form:

$$\lambda_k = T s_k; \quad \phi_k(t) = \frac{1}{\sqrt{T}} e^{i\omega_k t} \quad (k = \pm 1, \pm 2, \dots) \quad (20)$$

where the eigenfunctions have been normalised with respect to the inner product defined in Eq. (11), i.e.,  $\|\phi_k\| = 1$ ,  $k \in \mathbb{N}$ .

The POD modes of a mean-square-periodic process are denumerable infinite and correspond to the Fourier modes. Accordingly, any realisation of the process  $v(t)$  can be represented by particularising Eqs. (13) and (14) as:

$$v(t) = \frac{1}{\sqrt{T}} \sum_{k=-\infty}^{\infty} e^{i\omega_k t} x_k \quad (21)$$

$$x_k = \frac{1}{\sqrt{T}} \int_{-T/2}^{T/2} e^{-i\omega_k t} v(t) dt \quad (k = \pm 1, \pm 2, \dots) \quad (22)$$

Again, the PC of the process,  $x_k$ , are uncorrelated with each other according to Eq. (9). The spectral representation formula for the covariance function remains expressed by Eq. (18) that combined with Eq. (20) can assume the form given in Eq. (15).

In the general case of non-periodic stationary processes, the search for the POD modes  $\phi(t)$  should be performed letting  $t \in (-\infty, \infty)$  and leads to mathematical difficulties of formal and technical nature. Formal difficulties are related to the definition of the functionals  $J$  and  $J_1$  (Eqs. (1)-(3)) and may be circumvented through the concept of generalised functions (Kanwal 1983); technical difficulties arise in the calculation of the integral of Eq. (12) (over the interval  $(-\infty, \infty)$ ) that may not converge.

An elegant way-out (Lumley 1970) consists in writing Eq. (12) in a weak form multiplying both sides by a test function  $u(t_1)$  and integrating over  $t_1$ :

$$\int_{-\infty}^{\infty} \int_{-\infty}^{\infty} u^*(t_1) C_v(t_1, t_2) \phi(t_2) dt_2 dt_1 = \lambda \int_{-\infty}^{\infty} u^*(t_1) \phi(t_1) dt_1 \quad (23)$$

Eq. (23) has the same meaning of Eq. (12) provided that it can be fulfilled for any choice of the test function  $u$  within a suitable space of functions that are exponentially decreasing at infinity (Lumley 1970).

Introducing the condition of stationarity through Eq. (16), Eq. (23) can be rewritten as:

$$\int_{-\infty}^{\infty} u^*(t_1) \left( \int_{-\infty}^{\infty} C_v(\tau) \phi(t_1 + \tau) d\tau \right) dt_1 = \lambda \int_{-\infty}^{\infty} u^*(t_1) \phi(t_1) dt_1 \quad (24)$$

Eq. (24) can be transformed into the frequency (or wave-number) domain through the Parseval theorem (e.g. Priestley 1981), making use of the properties of the convolution product. It yields:

$$\int_{-\infty}^{\infty} \hat{u}^*(\omega) (S_v(\omega) - \lambda) \hat{\phi}(\omega) d\omega = 0 \quad (25)$$

where  $\hat{u}$  and  $\hat{\phi}$  are the Fourier transform of  $u$  and  $\phi$ , respectively;  $S_v$  is the power spectral density function (psdf) of  $v(t)$  and  $\omega$  is the circular frequency. Here, the term frequency is adopted in a general sense without a specific physical meaning; in fact,  $\omega$  represents the actual circular frequency when the variable  $t$  stands for a time coordinate, while it indicates the wave number when  $t$  corresponds to a space coordinate. Moreover, the existence of the Fourier transform of  $\phi(t)$  as an ordinary function is not assured, thus  $\hat{\phi}(\omega)$  should be interpreted as a generalised function.

Since Eq. (25) must be fulfilled for any choice of the function  $\hat{u}$ , which surely exists as an ordinary function since  $u$  has been chosen among rapidly (enough) decreasing functions, any solution of Eq. (25) must be given in the form:

$$\lambda = \lambda(\omega') = S_v(\omega'); \quad \hat{\phi}(\omega) = \hat{\phi}(\omega, \omega') = \delta(\omega - \omega') \quad (26)$$

for any real parameter  $\omega'$ ;  $\delta$  is the Dirac function. The POD modes can be obtained by an inverse Fourier transform of Eq. (26) and depend, as well as the eigenvalues, on the real parameter  $\omega'$ .

$$\phi(t, \omega') = e^{i\omega' t} \quad (\omega' \in \mathbb{R}) \quad (27)$$

Likewise in the case of periodic processes, the POD modes correspond to the Fourier modes; in this case, however, they are non-denumerable infinite (a mode for any value of the real parameter  $\omega'$ ). The POD eigenvalues correspond to the psdf  $S_v(\omega)$  and constitute a so-called continuous spectrum. Moreover, the eigenfunctions cannot be normalised, since their norm defined according to Eq. (11) diverges; it follows that the generalisation of Eq. (21) to represent the realisations of the process  $v(t)$  should be obtained introducing the Stieltjes integral (Priestley 1981):

$$v(t) = \int_{-\infty}^{\infty} e^{i\omega t} dY(\omega) \quad (28)$$

where  $Y(\omega)$  is a random process whose increments  $dY(\omega) = Y(\omega + d\omega) - Y(\omega)$  have order  $O(d\omega^{1/2})$  and are uncorrelated on non-overlapping intervals:

$$E[dY(\omega)dY^*(\omega')] = \begin{cases} S_v(\omega)d\omega & \text{if } \omega = \omega' \\ 0 & \text{otherwise} \end{cases} \quad (29)$$

Eq. (28) has deep analogies with Eq. (21), where the realisation of  $v(t)$  are represented by a sum

(an integral in Eq. (28)) of deterministic functions of time, the POD modes, modulated by random coefficients ( $x_k$  in Eq. (21),  $dY(\omega)$  in Eq. (28)). Such coefficients are uncorrelated with each other according to Eqs. (9) and (29), respectively. The circular frequency  $\omega$  assumes the role of a “continuous index” identifying the different modes.

The spectral representation of the covariance function (Eq. (15) for finite-energy processes) can be obtained by combining Eqs. (28) and (29), leading to the well-known Wiener-Khintchine (Priestley 1981) equation:

$$C_v(t_1, t_2) = \int_{-\infty}^{\infty} e^{i\omega t_1} e^{-i\omega t_2} S_v(\omega) d\omega \quad (30)$$

Again the analogy with the case of finite-energy processes and periodic processes is quite evident. In particular, it is worth noting that periodic processes and also more general discrete-spectrum processes can be represented in the framework offered by Eqs. (23)-(30) letting:

$$Y(\omega) = \sum_{k=-\infty}^{\infty} x_k H(\omega - \omega_k); \quad S(\omega) = \sum_{k=-\infty}^{\infty} s_k \delta(\omega - \omega_k) \quad (31)$$

where  $H$  is the unit-step function. For this reason, the definition of POD for mean-square periodic processes will not be explicitly addressed in the following, being interpreted as a particularisation of the treatment regarding continuous-spectrum processes.

The generalisation of the above concepts to the case of  $n$ -V processes (whose realisations have values in  $\mathbb{C}^n$ ) requires rewriting Eqs. (23)-(25) considering the functions  $\phi(t)$  and  $u(t)$  as having values in  $\mathbb{C}^n$ . In such a case Eq. (25) becomes:

$$\int_{-\infty}^{\infty} \hat{\mathbf{u}}^*(\omega) (\mathbf{S}_v(\omega) - \lambda \mathbf{I}) \hat{\phi}(\omega) d\omega = 0 \quad (32)$$

where  $\mathbf{S}_v(\omega)$  is the power spectral density matrix (psdm) of  $\mathbf{v}(t)$ ,  $\mathbf{I}$  is the  $n$ -order identity matrix and  $\hat{\mathbf{u}}$  is the Fourier transform of the test function  $\mathbf{u}$  with values in  $\mathbb{C}^n$ . Operating likewise for Eq. (25), it can be easily proved that POD eigenvalues and eigenvectors result:

$$\begin{aligned} \lambda &= \lambda_k(\omega) = \gamma_k(\omega) \\ \phi(t) &= \phi_k(t, \omega) = e^{i\omega t} \theta_k(\omega) \end{aligned} \quad (\omega \in \mathbb{R}, \quad k = 1, \dots, n) \quad (33)$$

where  $\gamma_k(\omega)$  and  $\theta_k(\omega)$  satisfy the eigenvalue problem:

$$\mathbf{S}_v(\omega) \theta_k(\omega) = \gamma_k(\omega) \theta_k(\omega) \quad (\omega \in \mathbb{R}, \quad k = 1, \dots, n) \quad (34)$$

and are referred to as spectral eigenvalues and eigenvectors, respectively (Solari and Carassale 2000).  $\mathbf{S}_v(\omega)$  is (Hermitian) symmetric and non-negative definite, thus all the eigenvalues are real and non-negative; the eigenvectors are orthogonal (or can be chosen as orthogonal in case of multiple eigenvalues) and are normalised, for any  $\omega$ , with respect to the inner product of Eq. (4).

Each mode, identified by the discrete index  $k$  and by the continuous parameter  $\omega$ , is constituted by a vector-valued function of  $t$ , whose components are harmonics with circular frequency  $\omega$  and amplitude determined by the components of the spectral eigenvector  $\theta_k$ . Adopting the base of the POD modes, the representation formula of Eq. (28) can be generalised as:

$$\mathbf{v}(t) = \int_{-\infty}^{\infty} \sum_{k=1}^n e^{i\omega t} \boldsymbol{\theta}_k(\omega) dY_k(\omega) \quad (35)$$

where the sum has been introduced to span the index  $k$  of the modes, while the increments of the processes  $Y_k(\omega)$  fulfil the relationship:

$$E[dY_h(\omega)dY_k^*(\omega')] = \begin{cases} \gamma_k(\omega)d\omega & \text{if } \omega = \omega' \text{ and } h = k \\ 0 & \text{otherwise} \end{cases} \quad (36)$$

Eq. (35) represents any realisation of the process  $\mathbf{v}(t)$  as an integral, over  $\omega$ , and a sum, over  $k$ , of deterministic functions, the POD modes  $\boldsymbol{\phi}(t, \omega) = \boldsymbol{\theta}_k(\omega)e^{i\omega t}$ , modulated by the random coefficients  $dY_k(\omega)$ .

The covariance matrix can be obtained combining Eqs. (35) and (36), leading to the spectral decomposition formula:

$$\mathbf{C}_v(t_1, t_2) = \int_{-\infty}^{\infty} \sum_{k=1}^n e^{i\omega(t_1-t_2)} \boldsymbol{\theta}_k(\omega)\boldsymbol{\theta}_k^*(\omega)\gamma_k(\omega)d\omega \quad (37)$$

The above treatment can be easily extended to include the case of  $m$ -D processes just letting  $t$ , and as a consequence  $\omega$ , be vectors in  $\mathbb{R}^m$ , updating consistently the integration domain in Eqs. (23)-(25), (28) and (30), and introducing an appropriate definition for the inner product  $(\omega, t)$ .

### 2.5. Representation of incompletely-stationary random processes

In the previous sections, the representation problem has been treated considering first the case of finite-energy processes and then the case of infinite-energy (in particular stationary) processes. In some practical applications, relevant random quantities depending on two parameters (say  $t$  and  $s$ ) can be modelled as random processes that are stationary with respect to one variable (e.g.  $t$ ) and non-stationary with respect to the other one (e.g.  $s$ ).

Let us consider a 2-D random process  $v(s, t)$ , whose realisation have values in  $\mathbb{C}$  and are defined on the domain  $s \in [a, b]$ ,  $t \in \mathbb{R}$ . Following the same procedure adopted for fully-stationary processes, Eq. (23) can be rewritten as:

$$\int_{-\infty}^{\infty} \int_{-\infty}^{\infty} \int_a^b \int_a^b u^*(s_1, t_1) C_v(s_1, s_2, t_1, t_2) \phi(s_2, t_2) ds_2 ds_1 dt_2 dt_1 = \lambda \int_{-\infty}^{\infty} \int_a^b u^*(s_1, t_1) \phi(s_1, t_1) ds_1 dt_1 \quad (38)$$

where the test-function  $u(s_1, t_1)$  (rapidly decreasing for  $|t_1|$  tending to infinity for any  $s_1$ ) has been introduced in order to assure the convergence of the integrals and  $C_v(s_1, s_2, t_1, t_2) = E[v(s_1, t_1) v^*(s_2, t_2)]$  is the covariance function of  $v(s, t)$ .

Introducing the stationarity condition and applying the Parseval theorem to both sides of Eq. (38) calculating the Fourier transform with respect to the variable  $t_1$ , it results:

$$\int_{-\infty}^{\infty} \int_a^b \hat{u}^*(s_1, \omega) \left( \int_a^b S_v(s_1, s_2, \omega) \hat{\phi}(s_2, \omega) ds_2 - \lambda \hat{\phi}(s_1, \omega) \right) ds_1 d\omega = 0 \quad (39)$$

where  $S_v(s_1, s_2, \omega)$  is the cpsdf of the processes  $v(s_1, t)$  and  $v(s_2, t)$ . Likewise for Eq. (32), the parenthesis in Eq. (39) contains an eigenvalue problem (or rather a set of eigenvalue problems

spanned by the parameter  $\omega$ ). In this case, however, the eigenvalue problem is a continuous one and gives rise to a set of denumerable infinite eigenfunctions. The solution of Eq. (39) can be deduced following the same principle already adopted for Eqs. (25), resulting:

$$\begin{aligned}\lambda &= \lambda_k(\omega) = \gamma_k(\omega) \\ \phi(s, t) &= \phi_k(s, t, \omega) = e^{i\omega t} \theta_k(s, \omega)\end{aligned}\quad (\omega \in \mathbb{R}, \quad k = N) \quad (40)$$

where, for any value of the parameter  $\omega$ ,  $\gamma_k(\omega)$  and  $\theta_k(s, \omega)$  are the solution of the continuous-type eigenvalue problem:

$$\int_a^b \mathcal{S}_v(s_1, s_2, \omega) \theta_k(s_2, \omega) ds_2 = \gamma_k(\omega) \theta_k(s_1, \omega) \quad (\omega \in \mathbb{R}, \quad k \in N) \quad (41)$$

where the eigenfunctions  $\theta_k(s, \omega)$  are assumed as normalised with respect to the inner product defined in Eq. (11).

The POD modes given in Eq. (40) constitute a set of non-denumerable infinite functions, identified by the parameters  $\omega'$  and  $k$ . Each POD mode is a scalar function of  $s$  and  $t$ , and can be idealised as a Fourier mode (with respect to the dimension  $t$ ) modulated through the eigenfunctions  $\theta_k(s, \omega)$  along the dimension  $s$ . Adopting the POD modes as a base, the process  $v(s, t)$  can be represented as:

$$v(s, t) = \int_{-\infty}^{\infty} \sum_{k=1}^{\infty} e^{i\omega t} \theta_k(s, \omega) dY_k(\omega) \quad (42)$$

where the increments  $dY_k(\omega)$  satisfy the orthogonality condition of Eq. (36). Applying the definition of covariance function to Eq. (42), and making use of the orthogonality of the modes, the spectral decomposition of the covariance function results:

$$C_v(s_1, s_2, t_1, t_2) = \int_{-\infty}^{\infty} \sum_{k=1}^{\infty} e^{i\omega(t_1 - t_2)} \theta_k(s_1, \omega) \theta_k^*(s_2, \omega) \gamma_k(\omega) d\omega \quad (43)$$

Eqs. (38)-(43) can be easily generalised to the case of the representation of a process  $v(s, t)$  whose realisations have values in  $\mathbb{C}^n$ ,  $t \in \mathbb{R}^m$  and  $s$  belongs to a compact domain in  $\mathbb{R}^p$  on which the realisations of  $v$  are square-integrable for any  $t$ . In this case, the above equations remain valid just updating the integration domains and introducing the pertinent definition for inner and outer products.

## 2.6. Linear transformations of $n$ -V processes

Sections 2.3 to 2.5 were devoted to the derivation of POD-based representation formulae for different classes of random processes. In general, such representations assumed the form of a series of deterministic functions modulated by uncorrelated random variables. In the case of  $n$ -V processes, however, POD can be also interpreted as a linear transformation characterised by particular properties. In this sense, an  $n$ -V random process can be represented as the output of a linear filter defined according to two alternative techniques referred to as Covariance Proper Transformation (CPT) and Spectral Proper Transformation (SPT) (Solari and Carassale 2000).

Let us consider an  $n$ -V random process  $\mathbf{v}(t)$  (whose realisations have values in  $\mathbb{C}^n$ ) and let us

represent it through the expression:

$$\mathbf{v}(t) = \sum_{k=1}^n \phi_k(t)x_k(t) = \mathbf{\Phi}(t)\mathbf{x}(t) \quad (44)$$

where  $\mathbf{\Phi}(t)=[\phi_1(t)\dots\phi_n(t)]$  and  $\mathbf{x}(t)=[x_1(t)\dots x_n(t)]^T$ . Eq. (44) can be reviewed as a generalisation of PCA (Eq. (7)) in which the dependence on  $t$  has been included. The vectors  $\phi_k(t)$  are the eigenvectors of the zero  $t$ -lag covariance matrix,  $\mathbf{C}_v(t, t)=E[\mathbf{v}(t)\mathbf{v}^*(t)]$ ; the corresponding eigenvalues  $\lambda_k(t)$ , in general dependent on  $t$ , provide the variance of the PC  $x_k(t)$ .

Having defined the representation formula (Eq. (44)) only on the base of the zero- $t$ -lag covariance matrix, the PC  $x_k$  are uncorrelated only for the zero  $t$ -lag, and their covariance matrix results:

$$\mathbf{C}_x(t_1, t_2) = E[\mathbf{x}(t_1)\mathbf{x}^*(t_2)] = \begin{cases} \mathbf{\Lambda}(t_1) & \text{if } t_1 = t_2 \\ \mathbf{\Phi}^*(t_1)\mathbf{C}_v(t_1, t_2)\mathbf{\Phi}(t_1) & \text{otherwise} \end{cases} \quad (45)$$

where  $\mathbf{\Lambda}(t)=\mathbf{diag}(\lambda_1(t),\dots,\lambda_n(t))$ . The vector of the PC  $\mathbf{x}(t)$  can be interpreted as an  $n$ -V process and Eq. (44) as a linear algebraic transformation.

Eq. (44) becomes particularly expressive for stationary processes, where it represents a  $t$ -invariant transformation, being  $\mathbf{\Phi}$  independent of  $t$ . In this case, it is referred to as CPT and results:

$$\mathbf{v}(t) = \sum_{k=1}^n \phi_k x_k(t) = \mathbf{\Phi}\mathbf{x}(t) \quad (46)$$

where the process  $\mathbf{v}(t)$  is represented as a sum of deterministic vectors modulated by the covariance PC  $x_k(t)$  whose covariance matrix is given by the relationship:

$$\mathbf{C}_x(\tau) = E[\mathbf{x}(t+\tau)\mathbf{x}^*(t)] = \begin{cases} \mathbf{\Lambda} & \text{if } \tau = 0 \\ \mathbf{\Phi}^*\mathbf{C}_v(\tau)\mathbf{\Phi} & \text{otherwise} \end{cases} \quad (47)$$

SPT is a  $t$ -invariant linear transformation whose definition is strictly correlated to the POD representation of the  $n$ -V stationary processes  $\mathbf{v}(t)$  (whose realisations are functions with values in  $\mathbb{C}^n$ ); they can be expressed as (Priestley 1981):

$$\mathbf{v}(t) = \int_{-\infty}^{\infty} e^{i\omega t} d\mathbf{V}(\omega) \quad (48)$$

where  $\mathbf{V}(\omega)$  is an orthogonal-increment process such that:

$$E[d\mathbf{V}(\omega)d\mathbf{V}^*(\omega')] = \begin{cases} \mathbf{S}_v(\omega)d\omega & \text{if } \omega = \omega' \text{ and } h = k \\ 0 & \text{otherwise} \end{cases} \quad (49)$$

The increment process  $d\mathbf{V}(\omega)$  can be expressed in terms of POD modes by comparing Eqs. (48) and (35), and exploiting the orthogonality of the Fourier modes; it results:

$$d\mathbf{V}(\omega) = \sum_{k=1}^n \boldsymbol{\theta}_k(\omega)dY_k(\omega) = \boldsymbol{\Theta}(\omega)d\mathbf{Y}(\omega) \quad (50)$$

where  $\boldsymbol{\Theta}(\omega)=[\boldsymbol{\theta}_1(\omega)\dots\boldsymbol{\theta}_n(\omega)]$  and  $\mathbf{Y}(\omega)=[Y_1(\omega)\dots Y_n(\omega)]^T$ . The matrix  $\boldsymbol{\Theta}(\omega)$  can be interpreted as the

frequency response function of the time-invariant linear transformation:

$$\mathbf{v}(t) = \mathcal{J}[\mathbf{y}(t)] \quad (51)$$

representing the process  $\mathbf{v}(t)$  as a linear mapping of the process  $\mathbf{y}(t)$  whose components  $y_k(t)$  are defined as:

$$y_k(t) = \int_{-\infty}^{\infty} e^{i\omega t} dY_k(\omega) \quad (52)$$

Such components are referred to as spectral PC of the process  $\mathbf{v}(t)$ , are uncorrelated for any  $t$ -lag (i.e., are incoherent) and their psdf is provided by the spectral eigenvalues  $\gamma_k(\omega)$  (Solari and Carassale 2000):

$$\mathbf{S}_v(\omega) = \Gamma(\omega) \quad (53)$$

being  $\mathbf{S}_v(\omega)$  the psdm of  $\mathbf{y}(t)$  and  $\Gamma(\omega) = \mathbf{diag}(\gamma_1(\omega), \dots, \gamma_n(\omega))$ . Combining Eqs. (36), (49) and (50), the psdm of  $\mathbf{v}(t)$  can be expressed through the factorisation:

$$\mathbf{S}_v(\omega) = \sum_{k=1}^n \boldsymbol{\theta}_k(\omega) \boldsymbol{\theta}_k^*(\omega) \gamma_k(\omega) = \boldsymbol{\Theta}(\omega) \Gamma(\omega) \boldsymbol{\Theta}^*(\omega) \quad (54)$$

According to SPT, the random process  $\mathbf{v}(t)$  is represented by a sum of incoherent terms constituted by vectors having fully coherent components.

Comparing Eqs. (48), (50), (52) and (46), it can be observed that, if the process  $\mathbf{v}(t)$  is stationary and if the matrix  $\boldsymbol{\Theta}$  do not depend on  $\omega$ , CPT and SPT become formally identical. Their identity, however, is not just formal since it can be demonstrated (Carassale 2005) that, if the spectral eigenvectors do not depend on frequency, then they coincide with the covariance eigenvectors,  $\boldsymbol{\Theta} = \boldsymbol{\Phi}$ , and the spectral PC coincide with the covariance PC,  $x_k = y_k$ .

SPT is explicitly expressed in the frequency domain through Eq. (50), which uses the eigenvector matrix  $\boldsymbol{\Theta}(\omega)$  as a frequency response function. The time-domain version of SPT is represented by the linear operator  $\mathcal{J}$  (Eq. (51)), whose expression can be obtained realising continuous or discrete-time state-space models as shown in Carassale (2005) and Chen and Kareem (2005), respectively.

## 2.7. Digital simulation of random processes

The above sections showed that POD provides a comprehensive framework for defining representation formulae for different classes of random processes. The basic concept is that a process is expressed as a sum of deterministic functions modulated by uncorrelated random amplitudes.

In the case of finite-energy processes, such a sum is composed by denumerable-infinite terms, thus a simulation formula can be obtained truncating the sum of Eq. (13) to a certain term  $n_c$ :

$$v(t) \simeq \sum_{k=1}^{n_c} \phi_k(t) \sqrt{\lambda_k} \xi_k \quad (55)$$

where the eigenvalues  $\lambda_k$  are considered as sorted in decreasing order and the coefficients  $\xi_k$  are zero-mean, unit-variance uncorrelated random variables, i.e.:

$$E[\xi_k] = 0; \quad E[\xi_h \xi_k^*] = \delta_{hk} \quad (56)$$

The series in Eq. (55) converges in the mean square as  $n_c$  tends to infinity, thus the target covariance function can be approximated with any arbitrary accuracy selecting a suitable value for  $n_c$ . Eq. (55) has been derived for the case of 1-V 1-D processes, however the general  $n$ -V  $m$ -D case can be tackled in the same fashion.

In the case of stationary (or incompletely-stationary) processes, the representation formula contains a sum of nondenumerable-infinite terms expressed through a Stieltjes integral. Considering first, for sake of simplicity, the case of 1-D 1-V processes, a simulation formula can be obtained by discretising the integral in Eq. (28) along a suitable sequence of frequency values  $\omega_j = j\Delta\omega$ , being  $\Delta\omega$  a suitable frequency step:

$$v(t) \approx \sum_{j=-n_\omega}^{n_\omega} e^{i\omega_j t} \sqrt{S_v(\omega_j)\Delta\omega} \xi_j \quad (57)$$

where  $n_\omega$  is the number of harmonics included in the simulation and  $\xi_j$  are random numbers generated according to Eqs. (56). It is worth noting that Eq. (57) corresponds to the representation formula developed for mean-square periodic processes (Eq. (21)), thus the process simulated by such a formula results periodic with period  $T = 2\pi/\Delta\omega$ .

The above treatment can be easily extended to the case of  $n$ -V random processes (Eqs. (35) and (36)), leading to the simulation formula:

$$v(t) \approx \sum_{j=-n_\omega}^{n_\omega} \sum_{k=1}^{n_s} e^{i\omega_j t} \theta_k(\omega_j) \sqrt{\gamma_k(\omega_j)\Delta\omega} \xi_{jk} \quad (58)$$

where  $n_s \leq n$  is the number of spectral eigenvectors retained in the representation and the coefficients  $\xi_{jk}$  satisfy conditions analogous to Eqs. (56), i.e.:

$$E[\xi_{jk}] = 0; \quad E[\xi_{ih}\xi_{jk}^*] = \delta_{ij}\delta_{hk} \quad (59)$$

Realisations of an incompletely-stationary process  $v(s, t)$  (Eq. (42)) can be simulated by an expression analogous to Eq. (58), in which the eigenfunctions  $\theta_k(s, \omega)$  take the part of the eigenvectors  $\theta_k(\omega)$ .

Eqs. (55)-(59) can be directly used to simulate Gaussian processes. In such a case, the simulation procedure can be defined as follows: 1-calculate eigenvalues and eigenfunctions of the covariance functions (eigenvectors of the psdm for stationary processes); 2-define the number of terms to be retained in the simulation formula on the base of convergence requirements; 3-simulate  $\xi_k$  (or  $\xi_{jk}$ ) as a set of Gaussian independent random variables.

In the case of non-Gaussian processes, the above procedure can be generalised as described by Phoon, *et al.* (2002), making use of an iterative scheme. According to such a technique, realisations of a random process  $v(t)$  with covariance function  $C_v$  and marginal distribution  $F_v$  can be simulated as follows: 1-calculate the eigenvalues and eigenfunctions of  $C_v$ ; 2-select the number of terms  $n_c$  to be retained in the representation; 3-simulate the coefficients  $\xi_k$  (or  $\xi_{jk}$ ) as  $F_v$ -distributed random number satisfying Eqs. (56) (such a condition assures the matching of the covariance function); 4-evaluate, by the statistical analysis of a set of realisations, the marginal distribution of the simulated process and of its PC obtained by Eq. (14); 5-update the probability distribution of the coefficients  $\xi_k$ ; 6-repeat points 4 and 5 until the convergence to the marginal distribution of  $v(t)$ .

### 3. Some applications

As drawing a general picture of the most important POD applications in wind engineering is practically not possible, this section focuses on the research activity at the University of Genova, illustrating some recent analyses, based on POD, of four relevant problems of the wind chain: modelling and simulation of stationary (Section 3.1) and non-stationary (Section 3.2) turbulence fields, the bluff-body aerodynamics of tall building models (Section 3.3), and the buffeting response of long-span bridges (Section 3.4). All the analyses have been revised to make their development homogeneous with the theoretical background depicted in Section 2.

#### 3.1. Double POD of turbulent velocity fields

Let  $s_1, s_2, s_3$  be a Cartesian reference system with origin in  $O$  on the ground;  $s_3$  is vertical and directed upwards. The wind velocity is a 3-component random vector depending on the space  $\mathbf{s} = [s_1 \ s_2 \ s_3]^T$  and on the time  $t$ ; thus, it is a 3-V 4-D process, in general non-stationary and non-homogeneous. Considering averaging time intervals within the spectral gap and aeolic phenomena at synoptic scale, the wind velocity can be decomposed into the sum of a mean part  $\bar{\mathbf{v}}(\mathbf{s}) = [\bar{v}_1(\mathbf{s}) \ \bar{v}_2(\mathbf{s}) \ \bar{v}_3(\mathbf{s})]^T$  (time averaged over a convenient interval) depending on space only and a zero-mean turbulent fluctuation  $\mathbf{v}(\mathbf{s}, t) = [v_1(\mathbf{s}, t) \ v_2(\mathbf{s}, t) \ v_3(\mathbf{s}, t)]^T$ ; this latter quantity is usually modelled as a 3-V 4-D Gaussian process, stationary with respect to  $t$ , non-homogeneous with respect to  $\mathbf{s}$ . Thus, it is characterized by the two-point psdm:

$$\mathbf{S}_v(\mathbf{s}, \mathbf{s}', \omega) = \begin{bmatrix} S_{11}(\mathbf{s}, \mathbf{s}', \omega) & S_{12}(\mathbf{s}, \mathbf{s}', \omega) & S_{13}(\mathbf{s}, \mathbf{s}', \omega) \\ S_{21}(\mathbf{s}, \mathbf{s}', \omega) & S_{22}(\mathbf{s}, \mathbf{s}', \omega) & S_{23}(\mathbf{s}, \mathbf{s}', \omega) \\ S_{31}(\mathbf{s}, \mathbf{s}', \omega) & S_{32}(\mathbf{s}, \mathbf{s}', \omega) & S_{33}(\mathbf{s}, \mathbf{s}', \omega) \end{bmatrix} \quad (60)$$

where  $S_{ij}(\mathbf{s}, \mathbf{s}', \omega)$  ( $i, j = 1, 2, 3$ ) is the cpsdf of  $v_i(\mathbf{s}, t)$  and  $v_j(\mathbf{s}', t)$ :

$$S_{ij}(\mathbf{s}, \mathbf{s}', \omega) = \sqrt{S_i(\mathbf{s}, \omega) S_j(\mathbf{s}', \omega)} \text{Coh}_{ij}(\mathbf{s}, \mathbf{s}', \omega) \quad (i, j = 1, 2, 3) \quad (61)$$

$S_i(\mathbf{s}, \omega) = S_{ii}(\mathbf{s}, \omega)$  is the psdf of  $v_i(\mathbf{s}, t)$ ,  $\text{Coh}_{ij}(\mathbf{s}, \mathbf{s}', \omega)$  is the coherence function (cohf) of  $v_i(\mathbf{s}, t)$  and  $v_j(\mathbf{s}', t)$ .

Let us consider a flat homogeneous terrain and  $\mathbf{s}, \mathbf{s}'$  within the internal boundary layer. The mean wind velocity is aligned with  $s_1$  and has intensity  $\bar{u}$ , i.e.,  $\bar{\mathbf{v}}(\mathbf{s}) = [\bar{u}(\mathbf{s}) 0 0]^T$ ;  $v_1, v_2, v_3$  are the longitudinal (along  $s_1$ ), lateral (along  $s_2$ ) and vertical (along  $s_3$ ) turbulence components;  $\mathbf{v}(\mathbf{s}, t)$  is a 3-V 4-D zero-mean Gaussian process, stationary with respect to  $t$ , homogeneous with respect to  $s_1$  and  $s_2$ , non-homogeneous with respect to  $s_3$ . In this case the psdf of  $v_i(\mathbf{s}, t)$  does not depend on  $s_1$  and  $s_2$ , while the coherence function of turbulence in two points  $\mathbf{s}, \mathbf{s}'$  with the same height  $s_3$  depends on their distance  $\|\mathbf{s} - \mathbf{s}'\|$  and on  $s_3$ .

The discretised turbulence field at  $N$  points in the space is a  $3N$ -V 1-D stationary process whose CPT and SPT are expressed by Eqs. (46) and (50), respectively. Carassale and Solari (2005) discussed the POD-based simulation of a turbulence field on a complex domain from a numeric viewpoint. Tubino and Solari (2005) showed the advantages of carrying out a two-step POD representation of the turbulence field, defined as Double POD; this method enables a conceptually rich interpretation of the physical phenomenon and involves relevant operative advantages whenever each POD step can be solved in closed form.

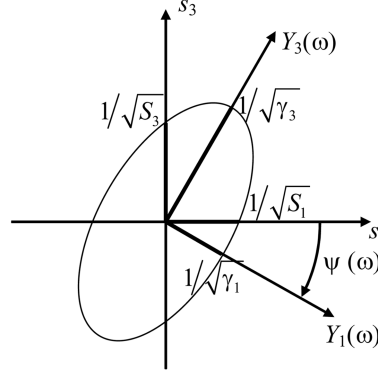


Fig. 1 Spectral principal components

With this aim, let us start with the analysis of the single-point turbulence vector  $\mathbf{v}(\mathbf{s}, t)$ ; it is a 3-V 1-D process, stationary with respect to  $t$ , where  $\mathbf{s}$  plays only the role of a parameter; its psdm is  $\mathbf{S}_v(\mathbf{s}, \omega) = \mathbf{S}_v(\mathbf{s}, \mathbf{s}, \omega)$  (Eq. (60)).

Applying Eq. (50), the SPT of  $\mathbf{v}(\mathbf{s}, t)$  is given by:

$$d\mathbf{V}(\mathbf{s}, \omega) = \mathbf{\Theta}(\mathbf{s}, \omega) d\mathbf{Y}(\mathbf{s}, \omega) = \sum_{k=1}^3 \boldsymbol{\theta}_k(\mathbf{s}, \omega) dY_k(\mathbf{s}, \omega) \quad (62)$$

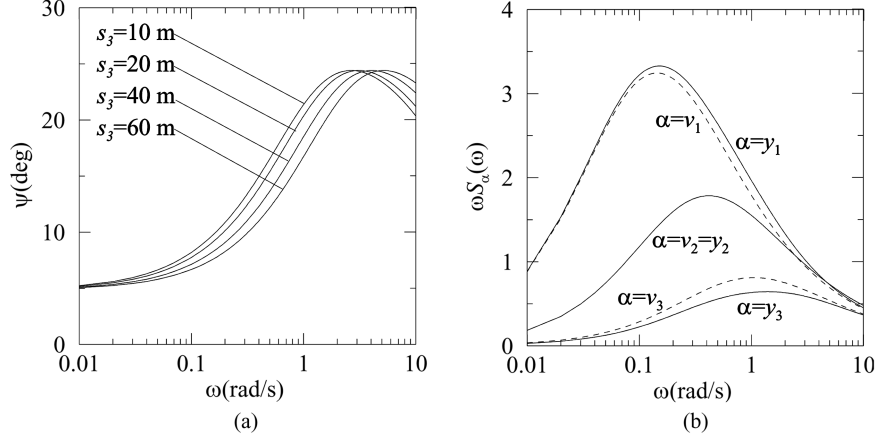
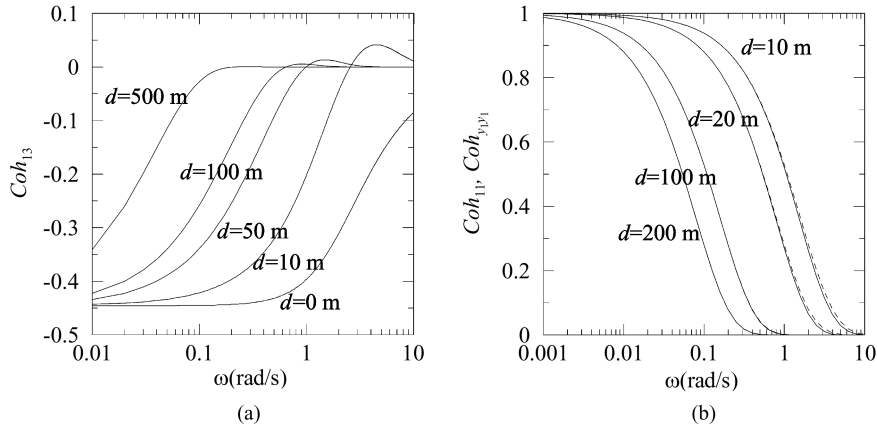
where  $\mathbf{\Theta}(\mathbf{s}, \omega) = [\boldsymbol{\theta}_1(\mathbf{s}, \omega) \boldsymbol{\theta}_2(\mathbf{s}, \omega) \boldsymbol{\theta}_3(\mathbf{s}, \omega)]$  is the matrix of the spectral eigenvectors;  $\mathbf{V}(\mathbf{s}, \omega)$  and  $\mathbf{Y}(\mathbf{s}, \omega)$  are 3-V complex-valued processes related to  $\mathbf{v}(\mathbf{s}, t)$  and to the spectral PC  $\mathbf{y}(\mathbf{s}, t)$  through Eqs. (48) and (52), respectively; the psdm of  $\mathbf{y}(\mathbf{s}, t)$  is the diagonal matrix of the spectral eigenvalues. Thus, for each position  $\mathbf{s}$  and for each frequency value  $\omega$ , the spectral eigenvectors identify a basis in  $\mathbb{R}^3$  or three orthogonal directions referred to as spectral principal directions. Each harmonic of  $y_k(\mathbf{s}, t)$  represents the Cartesian component along  $\boldsymbol{\theta}_k(\mathbf{s}, \omega)$  of the corresponding harmonic of  $\mathbf{v}(\mathbf{s}, t)$ .

It is worth noting that, under the classic assumption that  $v_2$  is uncorrelated with  $v_1$  and  $v_3$ ,  $v_2$  is a PC, i.e.,  $v_2 = y_2$ ; in such a case the SPT defines two PC,  $y_1$  and  $y_3$ , whose harmonics are rotated  $\psi(\omega)$  with respect to  $s_1$  and  $s_3$ , respectively (Fig. 1). In this relevant case, the spectral eigenvalues and eigenvectors can be determined in closed form (Solari and Tubino 2002). As an example (Solari and Tubino 2002), Fig. 2(a) shows typical diagrams of the angle  $\psi(\omega)$ ; Fig. 2(b) depicts the psdf of  $v_1, v_2, v_3$  (dashed lines), and of  $y_1, y_2, y_3$  (solid lines).

It can be proved that if  $v_1, v_2, v_3$  are assumed as uncorrelated with each other, then  $\mathbf{\Phi}(\mathbf{s}) = \mathbf{\Theta}(\mathbf{s}, \omega) = \mathbf{I}$  and the original turbulence components identify with the spectral PC, i.e.,  $\mathbf{v}(\mathbf{s}, t) = \mathbf{y}(\mathbf{s}, t)$ .

The definition of turbulence PC enables a conceptually rich representation of the single-point turbulence vector; moreover, if a statistical model for the two-point characterization of different turbulence components is not available (Solari and Piccardo 2001), this can be derived imposing that different PC, being uncorrelated at a single point, are uncorrelated also at different points; in such a way, explicit expressions of the two-point coh of distinct original turbulence components and of the same spectral PC can be obtained (Solari and Tubino 2002, Tubino and Solari 2005). These results complete both the turbulence models based on the original turbulence components and on the spectral PC.

As an example, Fig. 3(a) depicts the coh of  $v_1$  and  $v_3$  along a horizontal line orthogonal to the

Fig. 2 Rotation angle (a) and psdf (b) of  $v_1, v_2, v_3$  and  $y_1, y_2, y_3$ Fig. 3 Cohf of  $v_1$  and  $v_3$  (a) and of  $v_1$  and of  $y_1$  (b)

wind direction, for various distances  $d = |s_2 - s'_2|$ ; Fig. 3(b) compares the coh of  $y_1$  (solid lines) and of  $v_1$  (dashed lines).

Let us consider now the turbulence component  $\alpha(r, t)$  along a finite 1-D domain  $\mathcal{D}$  of length  $\ell$  and abscissa  $r$ , being  $\alpha = v_i$  or  $\alpha = y_i$  ( $i = 1, 2, 3$ );  $\alpha(r, t)$  is an 1-V 2-D zero-mean Gaussian process, stationary with respect to  $t$ , non-homogeneous with respect to  $r$ . Using Eq. (50), the SPT of  $\alpha(r, t)$  is given by (Solari and Carassale 2000):

$$dA(r, \omega) = \sum_{h=1}^{\infty} \mathfrak{G}_h(r, \omega) dZ_h(\omega) \quad (63)$$

where  $\mathfrak{G}_h(r, \omega)$  is the  $h$ -th eigenfunction of the cpsdf of  $\alpha(r, t)$ ,  $A(r, \omega)$  and  $Z_h(\omega)$  are complex-valued random processes with orthogonal increments, related to the turbulence component  $\alpha(r, t)$  and to the spectral PC  $z_h(t)$ , respectively; the psdf of  $z_h(t)$  is the  $h$ -th eigenvalue  $\gamma_h(\omega)$  of the cpsdf of  $\alpha(r, t)$  ( $h = 1, 2, \dots$ ).

The transformation defined by Eq. (63) is particularly convenient when the coh of  $\alpha(r, t)$  has exponential form; in this case, the spectral eigenvalues  $\gamma_h(\omega)$  and eigenfunctions  $\mathfrak{S}_h(r, \omega)$  can be obtained in closed form (Van Trees 1968, Carassale and Solari 2002, Tubino and Solari 2005).

If the original turbulence components are considered as uncorrelated, Eq. (63) can be adopted to represent each turbulence component  $\alpha = v_1, v_2, v_3$ . If otherwise the correlation among  $v_1, v_2, v_3$  is considered (as this is correct at least for  $v_1$  and  $v_3$ ), Eq. (63) can be applied to each PC  $\alpha = y_1, y_2, y_3$ . In this second case, the joint application of Eqs. (62) and Eq. (63) gives rise to the Double POD (Tubino and Solari 2005):

$$d\mathbf{V}(r, \omega) = \sum_{k=1}^3 \sum_{h=1}^{\infty} \boldsymbol{\theta}_k(r, \omega) \mathfrak{S}_{kh}(r, \omega) dZ_{kh}(\omega) \quad (64)$$

where  $\boldsymbol{\theta}_k(r, \omega) = \boldsymbol{\theta}_k(\mathbf{s}, \omega)$ ,  $\mathbf{s}$  being a point in  $\mathcal{D}$  at abscissa  $r$ ;  $\mathfrak{S}_{kh}(r, \omega)$  is the  $h$ -th eigenfunction of the cpsdf of  $y_k(r, t)$ ,  $Z_{kh}(\omega)$  is a complex-valued process with orthogonal increments related to the  $h$ -th spectral PC  $z_{kh}(t)$  of  $y_k(r, t)$ ; the psdf of  $z_{kh}(t)$  is the  $h$ -th eigenvalue  $\gamma_{kh}(\omega)$  of the cpsdf of  $y_k(r, t)$ . Embedding Eq. (64) into a Monte Carlo framework:

$$\mathbf{v}(r, t) \simeq 2\text{Re} \left[ \sum_{j=1}^{n_\omega} \sum_{k=1}^3 \sum_{h=1}^{n_i} \boldsymbol{\theta}_k(r, \omega_j) \mathfrak{S}_{kh}(r, \omega_j) \sqrt{\gamma_{kh}(\omega_j) \Delta\omega} \xi_{jkh} e^{i\omega_j t} \right] \quad (65)$$

where  $\text{Re}[\bullet]$  indicates the real part and  $\xi_{jkh}$  are complex-valued Gaussian random variables that satisfy conditions analogous to Eq. (59), i.e.,  $E[\xi_{jkh}] = 0$ ,  $E[\xi_{jkh} \xi_{rsm}^*] = \delta_{jr} \delta_{ks} \delta_{hm}$ .

It is worth noting that, if  $v_2$  is considered as uncorrelated with  $v_1$  and with  $v_3$ , and if the coh of the turbulence PC has an exponentially decreasing trend, then the Double POD in Eqs. (64) and (65) is defined analytically. In such a case, the digital simulation of the turbulence field only requires the Monte Carlo generation of  $\xi_{jkh}$ .

Fig. 4 shows some simulated time histories of  $v_1, v_2, v_3$  in two points at  $r=0$  and 40 m in the horizontal domain  $\mathcal{D}$ .

### 3.2. Non-stationary simulation of wind velocity fields

Independently of the method applied (Section 3.1), the simulation of stationary turbulence fields associated with aeolic phenomena at the synoptic scale is one of the most classical problems in wind

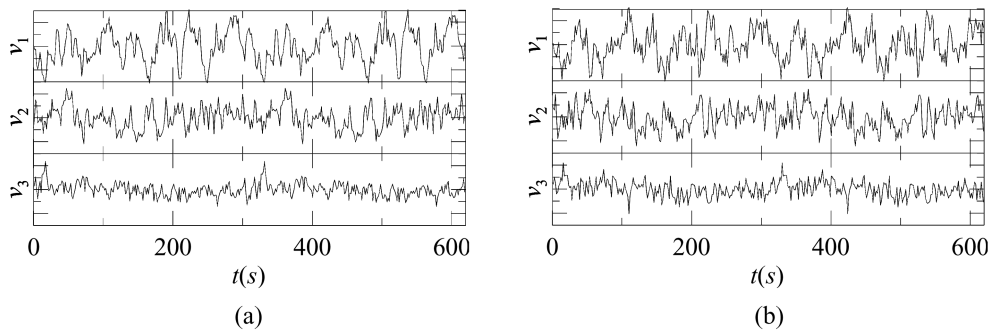


Fig. 4 Simulated time histories of the turbulence components

engineering. A less classical problem is the simulation of non-stationary turbulence fields associated with aeolic phenomena at the mesoscale (e.g. fronts, downbursts and tornadoes), or those experienced by a point-body moving along a spatial trajectory in a stationary turbulence field, crossing positions in which the wind flow has different statistical properties.

To deal with the second problem, let us consider the 3-V 4-D zero-mean Gaussian turbulence field  $\mathbf{v}(\mathbf{s}, t)$ , in general non-homogeneous with respect to  $\mathbf{s}$  and stationary with respect to  $t$ ; let  $\check{\mathbf{v}}(t) = \mathbf{v}(\check{\mathbf{s}}(t), t)$  be the turbulence field  $\mathbf{v}(\mathbf{s}, t)$  along the trajectory  $\mathbf{s} = \check{\mathbf{s}}(t)$  at the time  $t \in [0, T]$ . Likewise  $\mathbf{v}(\mathbf{s}, t)$ , also  $\check{\mathbf{v}}(t)$  is a Gaussian zero-mean random process but, in general, it is not stationary. The complete probabilistic representation of  $\check{\mathbf{v}}(t)$  is provided by its covariance matrix:

$$\mathbf{C}_{\check{\mathbf{v}}}(t_1, t_2) = E[\check{\mathbf{v}}(t_1) \check{\mathbf{v}}^T(t_2)] = \int_{-\infty}^{\infty} e^{i\omega(t_1 - t_2)} \mathbf{S}_{\check{\mathbf{v}}}(\check{\mathbf{s}}(t_1), \check{\mathbf{s}}(t_2), \omega) d\omega \quad (66)$$

Realizations of the process  $\check{\mathbf{v}}(t)$  can be expressed by Eq. (13) and simulated by Eq. (55), where  $\lambda_k$  and  $\phi_k(t)$  are, respectively, the eigenvalues and the eigenfunctions of  $\mathbf{C}_{\check{\mathbf{v}}}(t_1, t_2)$  in the domain  $[0, T]$ .

An application of this procedure consists in the representation and simulation of the non-stationary turbulence time-histories experienced by an aircraft during a landing or take-off route in proximity of an airport (Burlando, *et al.* 2005). This problem has special interest for the detection of critical conditions related to wind-shear phenomena induced by complex topography and for the occurrence of wind direction inversions, i.e., from headwind to tailwind, due to the presence of turbulent eddies.

The following results derive from a project aimed at studying and simulating the wind field in the neighbourhood of the Albenga airport in Italy. The applied procedure involves a three-step approach, namely the simulation of the mean wind field over a  $25 \times 30$  km wide domain by the mass-consistent computer program WINDS (Ratto, *et al.* 1994), the evaluation of the statistical properties of the turbulence field by the generalisation of the logarithmic law of the wall (Burlando, *et al.* 2005), and its simulation. Fig. 5 shows the topography of the macro-area (external rectangle) and of the micro-area (internal rectangle) selected to study the wind field numerically.

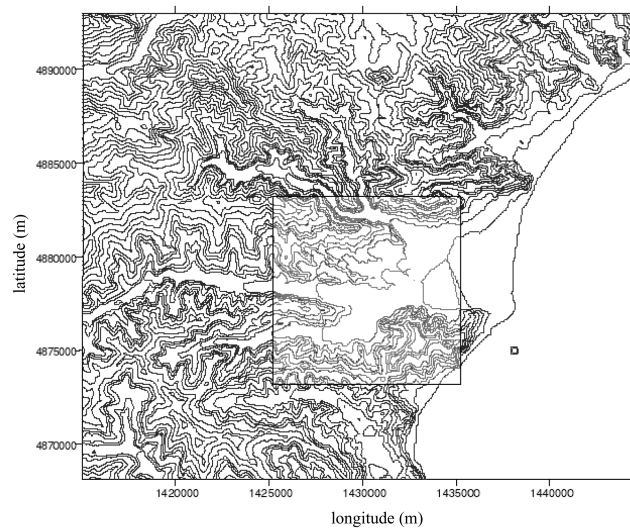


Fig. 5 Topographic map of the macro-area and of the micro-area

The three turbulence components  $v_1$ ,  $v_2$ ,  $v_3$  are assumed as Gaussian and uncorrelated with each other. Their probabilistic structure is defined by well-recognised spectral models that take into account the atmospheric thermal stratification; the spectral parameters are calibrated, in each point of the domain through the outcome of the mass-consistent simulation. Thanks to the aforementioned hypotheses, the three turbulence components can be simulated, independently with each other, by

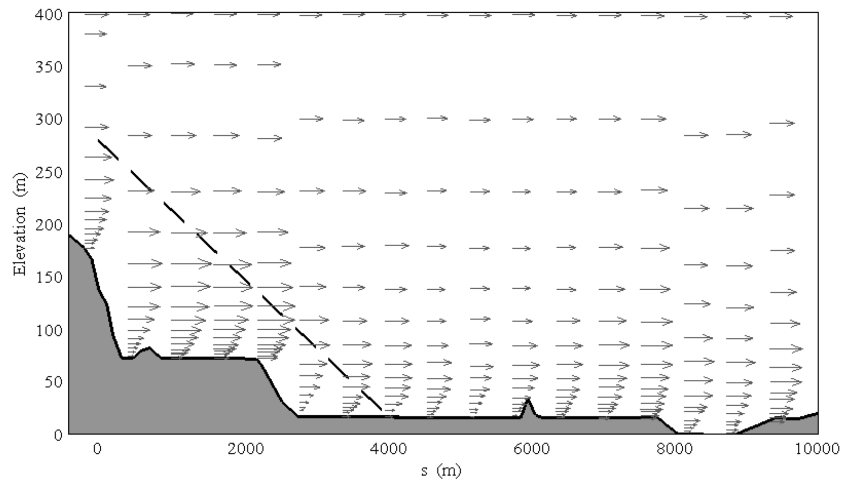


Fig. 6 Mean wind velocity in the glide-path plane

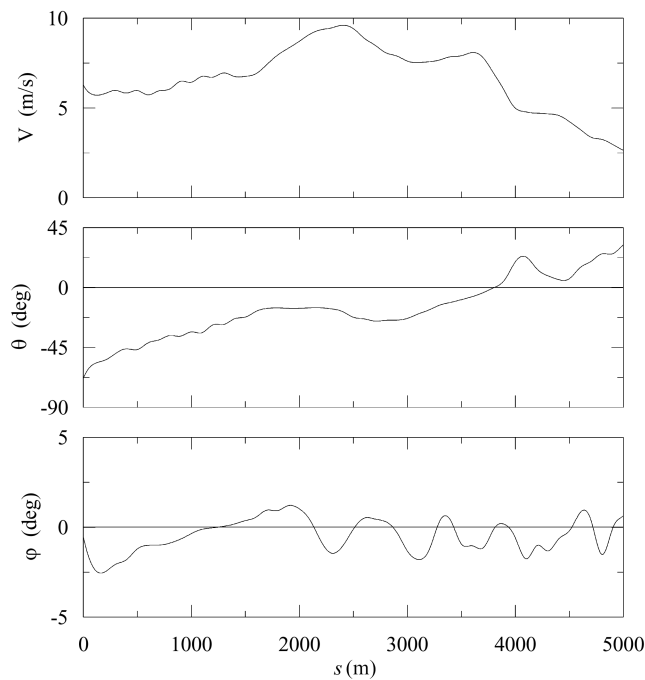


Fig. 7 Mean wind velocity: intensity  $V$ , angle with respect to the north  $\theta$ , angle with respect to the horizontal plane  $\phi$

means of Eq. (57), where  $\lambda_k$  and  $\phi_k$  are the eigenvalues and the eigenvectors of the (scalar-valued) covariance function evaluated through Eq. (66) for each turbulence component.

Fig. 6 shows a simulated wind field in the vertical plane containing the glide path (dashed line). The simulation has been initialised in order to obtain a suitable atmospheric stratification and a prescribed wind velocity and direction at the anemometer of the airport. Fig. 7 shows the mean wind velocity simulated along the glide path;  $V$  represents its intensity,  $\theta$  is its horizontal angle with respect to the north, and  $\varphi$  its vertical angle with respect to the horizontal plane. The graphs are plotted versus a horizontal abscissa  $s$  whose value  $s=4000$  m corresponds to the expected touch-down point.

Figs. 8 and 9 show, respectively, the eigenvalues and the eigenfunctions of the three turbulence components encountered by an airplane moving with a constant velocity of 150 km/h along the

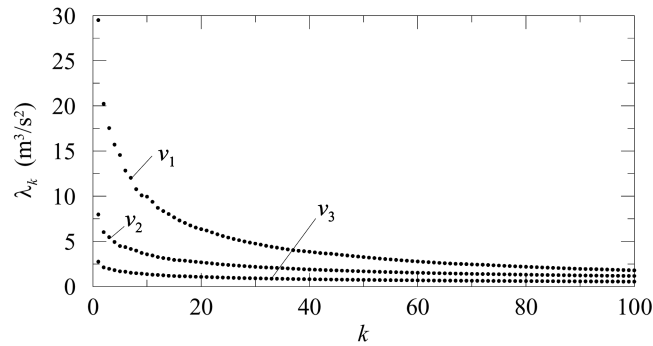


Fig. 8 Covariance eigenvalues of the three turbulence components

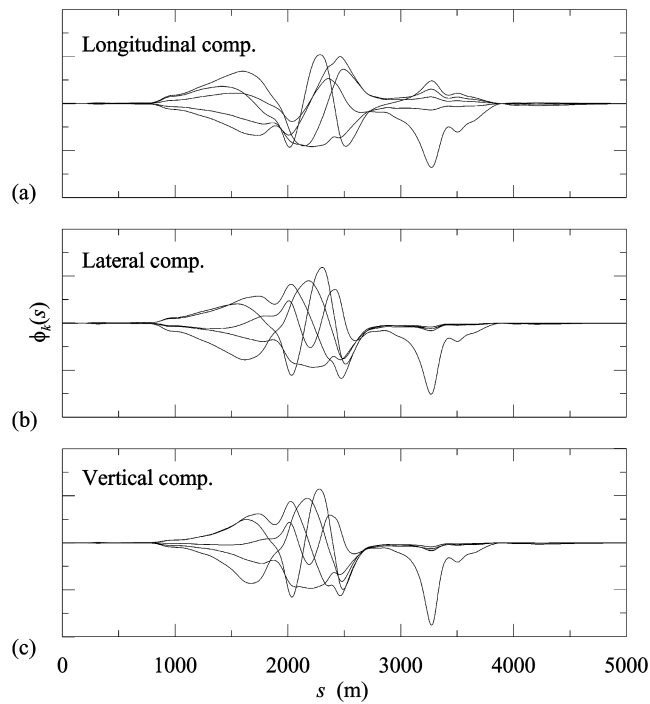


Fig. 9 Covariance eigenfunctions of  $\hat{v}_1(t)$  (a),  $\hat{v}_2(t)$  (b),  $\hat{v}_3(t)$  (c)

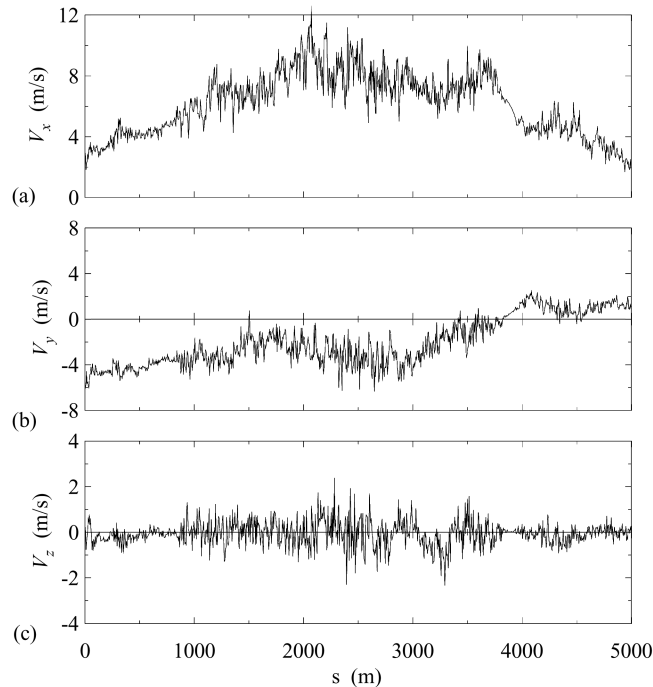


Fig. 10 Simulations of the nonstationary wind fluctuations  $V_x(t)$  (a),  $V_y(t)$  (b),  $V_z(t)$  (c)

glide path. Fig. 10 shows a simulation of the three Cartesian components  $V_x$  (west-east, along the glide path),  $V_y$  (south-north, orthogonal to the glide path),  $V_z$  (vertical) of the wind velocity field along the considered trajectory. It is apparent that the non-stationary characteristics of the realisations are greatly strengthened by the channelling effects, and the aircraft experiences the maximum wind intensity and turbulence in the middle of the landing descent.

### 3.3. Different POD representations of the wind forces on a tall building model

The POD of pressure fields and force distributions is a basic tool of bluff-body aerodynamics. It is applied to compact measured data, to detect coherent structures, and to identify reduced models of the aerodynamic loads. POD can be performed in a weak form, referred to as CPT, or in a strong form, referred to as SPT (Carassale, *et al.* 2004). Both can be applied to the original data or to some pre-processing of the original data, such as normalisation techniques, employed to emphasise some features of the phenomenon under investigation.

In order to discuss this issue, different POD approaches have been applied to the alongwind and crosswind forces on a tall building model submitted to boundary layer wind tunnel tests (Kikuchi, *et al.* 1997). The oncoming flow has a length scale 1:400 and corresponds to an urban exposure. The building model has a square section with side  $B=10$  cm, and height  $H=50$  cm. The wind velocity and the aerodynamic forces are represented by an orthogonal reference system  $s_1, s_2, s_3$  with origin in  $O$  on the wind tunnel floor;  $s_3$  is vertical, coincides with the building axis and is directed upwards. The mean wind velocity  $\bar{u}$ , aligned with  $s_1$ , is orthogonal to the windward face. The pressure was measured, simultaneously, by 500 taps uniformly distributed on the surface of the

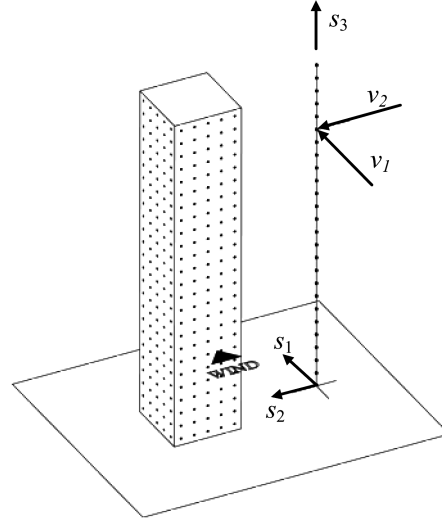


Fig. 11 Schematic representation of the experimental set-up

walls (Fig. 11). Alongwind (along  $s_1$ ) and crosswind (along  $s_2$ ) forces were obtained summing local pressures multiplied by the corresponding tributary areas at 25 levels, and non-dimensionalised by dividing all the components by  $0.5\rho\bar{u}^2(H)BH/25$ . A 50-V stationary process  $\mathbf{v}(t)$  has been defined staking in a vector the zero-mean fluctuation of alongwind and crosswind non-dimensional forces. The torsional moments around the vertical axis  $s_3$  (Kikuchi, *et al.* 1997) have not been considered for the sake of simplicity.

Fig. 12 shows the covariance eigenvalues  $\lambda_k$  (a), the psdf of the first four covariance PC  $x_k(t)$  as functions of the reduced frequency  $f=B\omega/2\pi\bar{u}(H)$  (b), the alongwind (c) and crosswind (d)

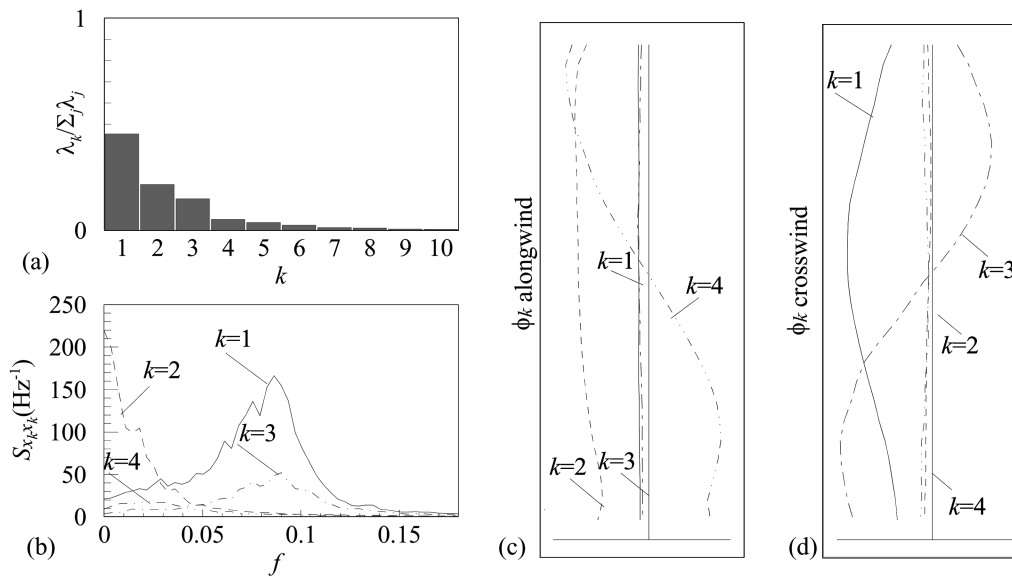


Fig. 12 CPT eigenvalues (a), psdf of CPT principal components (b) and CPT eigenvectors (c,d)

components of the corresponding covariance eigenvectors  $\phi_k$ . The covariance eigenvalues  $\lambda_k$  vanish quite rapidly on increasing mode  $k$ . The first and third modes contribute almost entirely to the crosswind force (Fig. 12(d)); since their harmonic content is concentrated around  $f \approx 0.085$ , such modes are mainly related to vortex shedding (Fig. 12(b)). The second and fourth modes are almost entirely in the alongwind direction (Fig. 12(c)) and refer to the buffeting action of the longitudinal turbulence (Fig. 12(b)).

Fig. 13 shows the first four spectral eigenvalues. The first one is much larger than the others and is characterised by two dominant frequency contents: the first, in the low frequency range, depends on turbulence buffeting; the second, around  $f \approx 0.085$ , corresponds to vortex shedding. Fig. 14 shows the amplitudes of the first two spectral modes at  $f=f_1, \dots, f_4$ ; black and white circles denote, respectively, alongwind and crosswind components. At  $f=f_1$ , the first and second modes represent alongwind and crosswind forces, respectively. At  $f=f_2$ , the first and second eigenvalues get close to each other and realise a veering; in that case, the first and second modes have similar amplitudes in both alongwind and crosswind directions. At  $f=f_3$ , due to the power supplied by vortex shedding, both modes are associated to pure crosswind forces. This situation persists on increasing the reduced frequency ( $f=f_4$ ).

Fig. 15 shows the recomposition of the standard deviations of  $\mathbf{v}(t)$ , respectively at levels 17 and

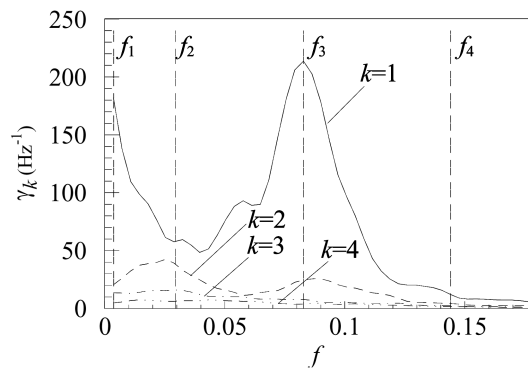


Fig. 13 SPT eigenvalues

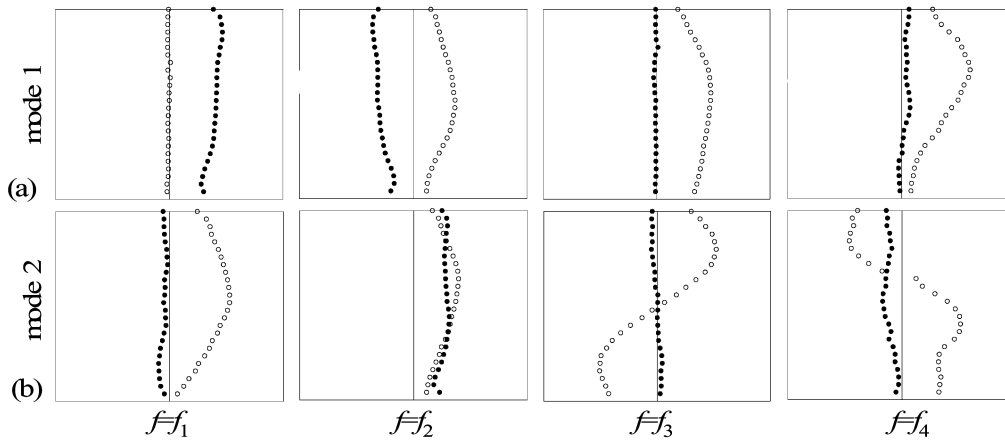


Fig. 14 Amplitudes of first (a) and second (b) SPT eigenvectors

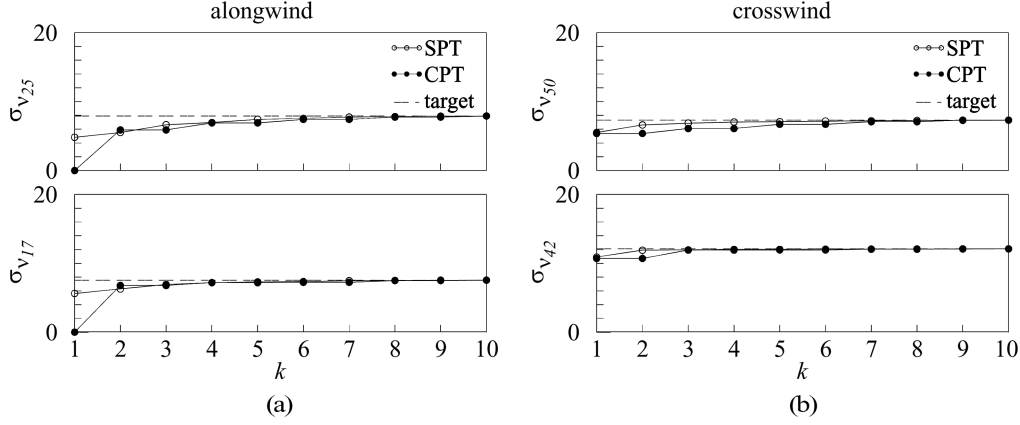


Fig. 15 CPT and SPT recomposition of the rms values of loading

25. Summing the contribution of POD modes, such values converge to the target measurements. However, convergence is faster at level 17, where few modes capture the overall loading mechanisms. Moreover, CPT converges more slowly than SPT. In fact, while CPT modes tend to be linked with one specific mechanism, each SPT mode refers to different phenomena in different frequency ranges. So, changing the frequency, each SPT mode is able to capture more excitation mechanisms and SPT may represent the target process using less modes than CPT. It is questionable, however, that this advantage may counterbalance, in bluff-body aerodynamics, the growing complexity involved by SPT with respect to CPT.

Let us express  $\mathbf{C}_v(0)$  and  $\mathbf{S}_v(\omega)$  as:

$$\mathbf{C}_v(0) = \mathbf{R}_c \hat{\mathbf{C}}_v(0) \mathbf{R}_c; \quad \mathbf{S}_v(\omega) = \mathbf{R}_s(\omega) \hat{\mathbf{S}}_v(\omega) \mathbf{R}_s(\omega) \quad (67)$$

where  $\mathbf{R}_c = \mathbf{diag}(\sigma_1, \dots, \sigma_n)$  and  $\mathbf{R}_s = \mathbf{diag}(S_{11}(\omega), \dots, S_{nn}(\omega))^{1/2}$ ,  $\sigma_i$  and  $S_{ii}(\omega)$  being the standard deviation and the psdf of  $v_i(t)$  ( $i=1, \dots, n$ ), respectively; the  $i, j$ -th terms of  $\hat{\mathbf{C}}_v(0)$  and  $\hat{\mathbf{S}}_v(\omega)$  are the correlation coefficient and the coh of  $v_i(t)$  and  $v_j(t)$  ( $i, j=1, \dots, n$ ), respectively. It follows that, while  $\mathbf{C}_v(0)$  and  $\mathbf{S}_v(\omega)$  contain a full information on the energy content of  $\mathbf{v}(t)$ ,  $\hat{\mathbf{C}}_v(0)$  and  $\hat{\mathbf{S}}_v(\omega)$  retain only a description of its correlation structure. Thus, CPT and SPT applied to  $\hat{\mathbf{C}}_v(0)$  and  $\hat{\mathbf{S}}_v(\omega)$  provide an interpretation of the physical mechanisms which underlie the correlation. Moreover, while the POD of  $\mathbf{v}(t)$  based on  $\mathbf{C}_v(0)$  and  $\mathbf{S}_v(\omega)$  allows an optimal reconstruction of the original process, the POD of  $\mathbf{v}(t)$  based on  $\hat{\mathbf{C}}_v(0)$  and  $\hat{\mathbf{S}}_v(\omega)$  does not imply the same property.

Fig. 16 shows the eigenvalues  $\hat{\lambda}_k$  of  $\hat{\mathbf{C}}_v(0)$  (a) and the eigenvalues  $\hat{\gamma}_k$  of  $\hat{\mathbf{S}}_v(\omega)$  (b). On increasing mode  $k$ , the eigenvalues  $\hat{\lambda}_k$  of  $\hat{\mathbf{C}}_v(0)$  vanish less rapidly than the eigenvalues  $\lambda_k$  of  $\mathbf{C}_v(0)$  (Fig. 12(a)). The first spectral eigenvalue of  $\hat{\mathbf{S}}_v(\omega)$  does not prevail over the higher ones as in Fig. 13. The eigenvalue related to the first alongwind mode (indicated in Fig. 16(b) by black circles) is characterised by the typical decay of the coh of longitudinal turbulence; the eigenvalue related to the first crosswind mode (indicated by white circles) is characterised by the typical pattern of the coh of vortex shedding.

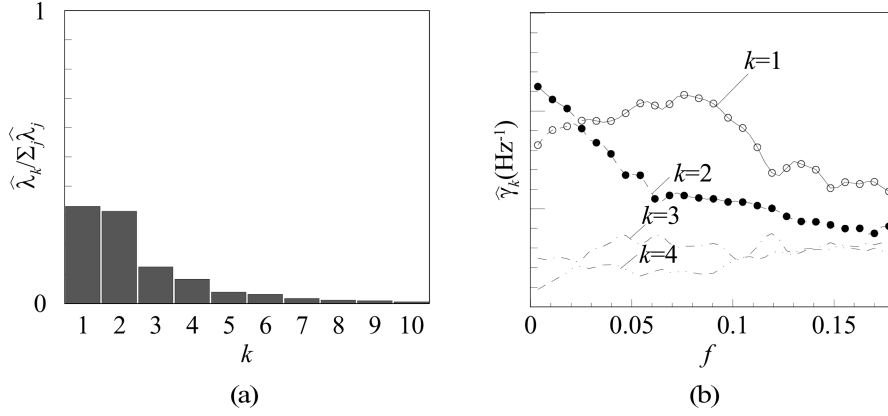


Fig. 16 CPT (a) and SPT (b) eigenvalues (normalized)

Finally, it is rather obvious that the CPT and SPT recompositions of the standard deviation based on the normalisation procedure described above involve a slower convergence than that exhibited by the POD application to the original process (Fig. 15).

### 3.4. DMT and buffeting response of long-span bridges

The equation of motion of an  $M$ -DOF linear structure is usually solved by applying the principal transformation rule:

$$\mathbf{q}(t) = \Psi \mathbf{p}(t) = \sum_{j=1}^M \boldsymbol{\psi}_j p_j(t) \quad (68)$$

where  $\mathbf{q}(t)$  is the Lagrangian displacement vector,  $\Psi = [\boldsymbol{\psi}_1 \dots \boldsymbol{\psi}_M]$  is the structural modal matrix,  $\boldsymbol{\psi}_1, \dots, \boldsymbol{\psi}_M$  are the orthonormal eigenvectors of structure, i.e.,  $\Psi^T \mathbf{M} \Psi = \mathbf{I}$ ;  $\mathbf{p}(t)$  is the vector of the structural principal coordinates, i.e., the image of  $\mathbf{q}(t)$  in the principal space.

If the structure has classical vibration modes Eq. (68) de-couples the equations of motion in the principal space:

$$\ddot{p}_j(t) + 2\zeta_j \omega_j \dot{p}_j(t) + \omega_j^2 p_j(t) = \boldsymbol{\psi}_j^T \mathbf{f}(t) \quad (j = 1, \dots, M) \quad (69)$$

$\omega_j$  and  $\zeta_j$  being the  $j$ -th natural circular frequency and damping ratio, respectively,  $\mathbf{f}(t) = \mathbf{A}\mathbf{v}(t)$  being the loading vector, where  $\mathbf{v}(t)$  is an  $n$ -V zero-mean Gaussian stationary random process and  $\mathbf{A}$  is an  $M \times n$  deterministic matrix. Sorting the natural circular frequencies in increasing order, the structural modal truncation consists in approximating the response (Eq. (68)) considering only a limited number  $M_t < M$  of structural modes.

Let us apply the SPT of  $\mathbf{v}(t)$ . Replacing Eq. (50) into the frequency domain counterpart of Eq. (69) yields:

$$dP_j(\omega) = H_j(\omega) \sum_{k=1}^n D_{jk}(\omega) dY_k(\omega) \quad (j = 1, \dots, M) \quad (70)$$

where  $P_j(\omega)$  and  $Y_k(\omega)$  are complex-valued processes with orthogonal increments related to  $p_j(t)$  and

to the spectral PC  $y_k(t)$ , respectively;  $H_j(\omega) = (-\omega^2 + 2i\zeta_j\omega_j\omega + \omega_j^2)^{-1}$  is the  $j$ -th complex frequency response function;  $D_{jk}(\omega) = \Psi_j^T \mathbf{A} \Theta_k(\omega)$  is the  $j, k$ -th term of  $\mathbf{D}(\omega) = \Psi^T \mathbf{A} \Theta(\omega)$ , referred to as the cross-modal participation spectral matrix. Thus,  $D_{jk}(\omega)$  is a participation factor which quantifies the influence of the  $k$ -th loading spectral mode on the  $j$ -th structural mode.

Several terms of the matrix  $\mathbf{D}$  are negligible. Due to the structural modal truncation, only  $M_i < M$  structural modes contribute to response. Due to spectral modal truncation, only  $n_s < n$  spectral modes contribute to the external load. Due to cross-modal orthogonality property, several  $k$  structural modes are quasi-orthogonal to several  $j$  loading modes with respect to  $\mathbf{A}$ , i.e.,  $D_{jk} \simeq 0$ . Thus, combining Eqs. (50) and (69), the structural response is expressed by a double linear combination of few structural modes and few loading modes referred to as Double Modal Transformation (DMT) (Solari and Carassale 2000, Carassale, *et al.* 2001).

The psdm of  $\mathbf{q}(t)$  and  $\mathbf{p}(t)$  are given by:

$$\mathbf{S}_{\mathbf{q}}(\omega) = \Psi \mathbf{S}_{\mathbf{p}}(\omega) \Psi^T; \quad \mathbf{S}_{\mathbf{p}}(\omega) = \mathbf{H}(\omega) \mathbf{D}(\omega) \Gamma(\omega) \mathbf{D}^*(\omega) \mathbf{H}^*(\omega) \quad (71)$$

where  $\mathbf{H}(\omega) = \text{diag}(H_1(\omega), \dots, H_M(\omega))$ ,  $\Gamma(\omega)$  is the diagonal matrix of the spectral eigenvalues, i.e., the psdf of the spectral PC  $y_k(t)$ .

As an example of special interest, DMT was applied to the gust buffeting of long-span bridges (Tubino and Solari 2007). The Messina Strait Bridge, currently under design, provides a unique opportunity for pointing out the potentialities of this approach. The bridge has a total length of 3.666 m, and a suspended main span of 3.300 m. The deck is schematised by a finite element model with 118 nodes along the axis; the position of the nodes and the vectors of the wind velocity are represented by an orthogonal reference system  $s_1, s_2, s_3$  with origin in  $O$  on the ground at the Sicily side;  $s_3$  is vertical and directed upwards;  $s_2$  lies in the symmetry plane of the bridge. Each node has 3-DOF, the lateral and vertical displacements,  $q_1$  (along  $s_1$ ) and  $q_3$  (along  $s_3$ ), and the torsional rotation  $q_\phi$  (around  $s_2$ ) (Fig. 17). The mean wind velocity is aligned with  $s_1$ ; the deck is subjected to the longitudinal (along  $s_1$ ) and vertical (along  $s_3$ ) turbulence components,  $v_1(t)$  and  $v_3(t)$ , treated as uncorrelated for the sake of simplicity. Thus,  $\mathbf{q}(t)$  is a vector of  $M=118 \times 3=354$  components;  $\mathbf{v}(t) = [\mathbf{v}_1(t)^T \ \mathbf{v}_3(t)^T]^T$  lists  $n=118 \times 2=236$  turbulence components;  $\mathbf{A} = [\mathbf{A}_1 \ \mathbf{A}_3]$  is an aerodynamic matrix whose terms are evaluated by quasi-steady theory and sectional model wind tunnel tests. It follows that Eq. (50) can be applied separately to the vectors  $\mathbf{v}_1(t)$  and  $\mathbf{v}_3(t)$ ,  $\mathbf{D}(\omega) = [\mathbf{D}_1(\omega) \ \mathbf{D}_3(\omega)]$ ,  $\mathbf{D}_1(\omega) = \Psi^T \mathbf{A}_1 \Theta_1(\omega)$  and  $\mathbf{D}_3(\omega) = \Psi^T \mathbf{A}_3 \Theta_3(\omega)$ ;  $\Theta_1(\omega)$  and  $\Theta_3(\omega)$  are the spectral eigenvectors of  $\mathbf{v}_1(t)$  and  $\mathbf{v}_3(t)$ , respectively.

Fig. 18(a) shows the first 8 structural modes of vibration,  $\Psi_1, \dots, \Psi_8$ , and the related natural frequencies  $n_1, \dots, n_8$ : solid, dashed and dash-dotted lines denote longitudinal, vertical and torsional components, respectively. It is worth notice that, due to bridge flexibility,  $n_{30}=0.177$  Hz. Fig. 18(b) shows the first 4

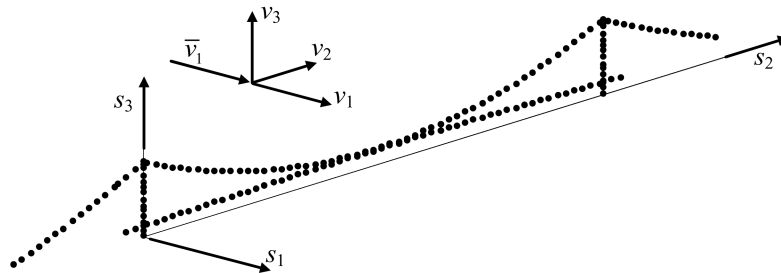


Fig. 17 Messina Straits Bridge schematization

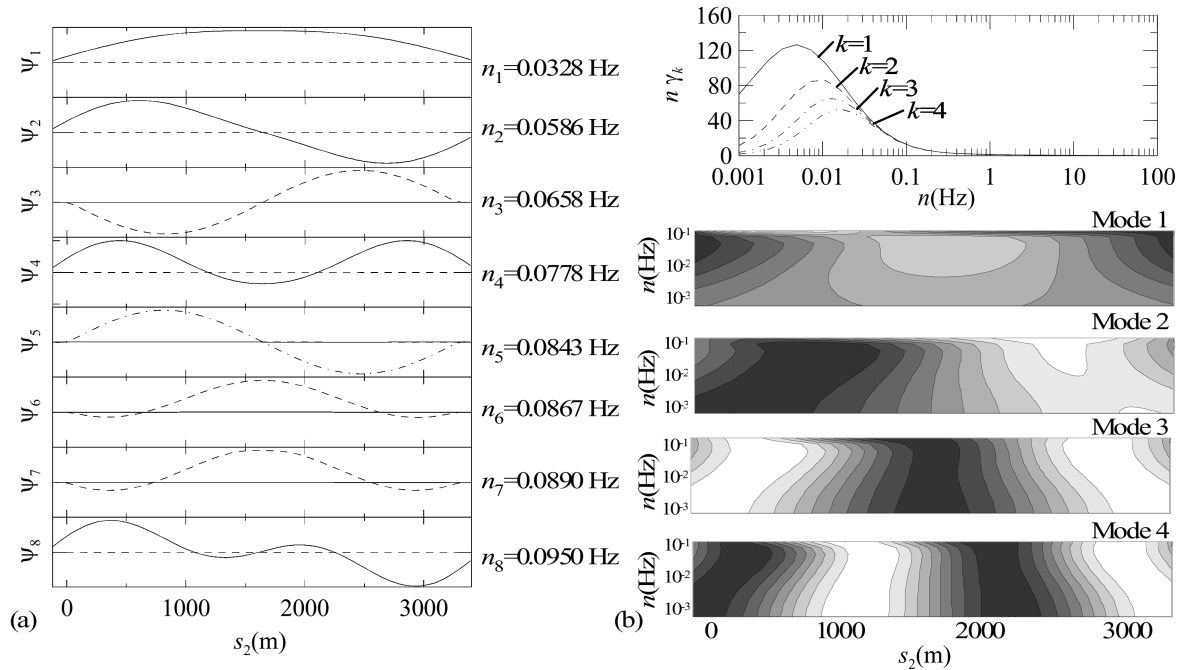


Fig. 18 Structural (a) and longitudinal turbulence (b) modes

spectral eigenvalues and eigenvectors of  $\mathbf{v}_1(t)$ . The diagrams correspond to  $n < 0.3$  Hz and show that, in this frequency range, the turbulence modes are characterised by a limited frequency dependence; instead, on increasing  $n$ , their shape tends to change with the frequency in a more relevant way.

Fig. 19 shows the cross-modal participation coefficients related to  $v_1$  (a) and  $v_3$  (b), for the first 30

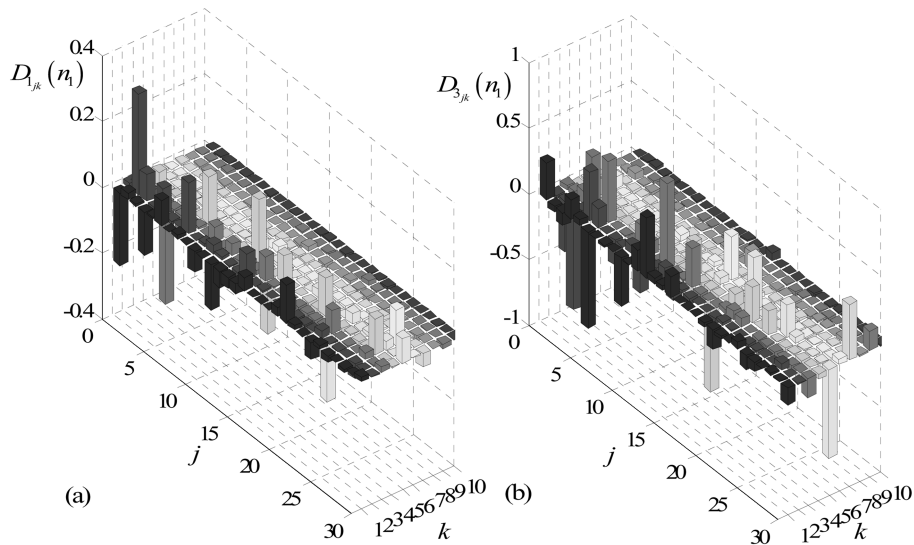


Fig. 19 Cross-modal participation coefficients: (a)  $v_1$  (b)  $v_3$

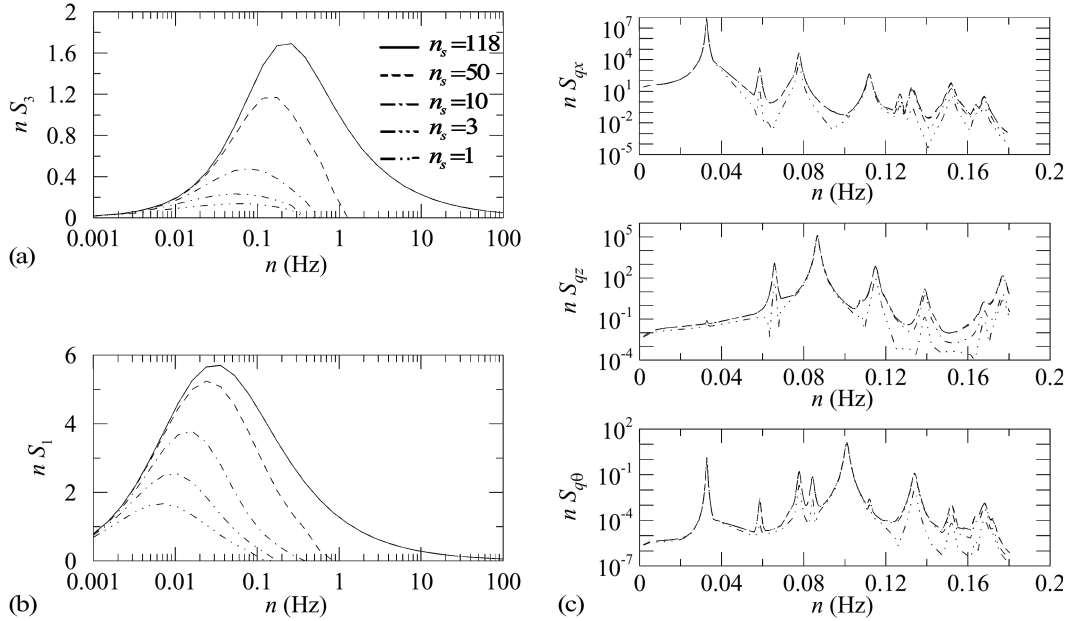


Fig. 20 Reconstruction of  $v_1$  (a), of  $v_3$  (b) and of the structural response (c) at the mid-span

modes of vibration, at  $n=n_1$ . The similarity of structural and turbulence modal shapes makes many structural modes quasi-orthogonal to many turbulence modes; as a result, several terms of the matrix  $\mathbf{D}$  vanish, and few turbulence modes excite few structural modes.

Fig. 20 shows the psdf of  $v_1$  (a), of  $v_3$  (b), and of the generalised displacements (c) at the mid-span, evaluated considering an increasing number of turbulence modes ( $n_s=1, 3, 10, 50, 118$ ). Fig. 20(a, b) shows that in the low frequency range few modes are enough to represent the turbulence; instead, in the high frequency range many modes, in principle all, are necessary to reproduce its harmonic content. On the other hand, Fig. 20(c) shows that the psdf of the response is well reproduced even representing the turbulence by a small number of modes.

Based on these considerations, let us define the effective turbulence as that part of the actual turbulence which really influences the structural response, i.e., the turbulence reconstructed using only the necessary POD modes, in this case the first three modes.

Fig. 21(a) shows the psdf of the longitudinal effective turbulence multiplied by the frequency; it is apparent that its harmonic content is concentrated in the low frequency range ( $n < 0.1$  Hz). Thus, time domain simulations can be carried out adopting time steps much wider than those normally used, e.g.  $\Delta t = 0.1$  s, without any relevant underestimation of the buffeting response. Moreover, since turbulence eigenvectors are almost independent of  $n$  for  $n < 0.1$  Hz (Fig. 18(b)), they can be approximated by a constant value; thus, SPT coincides with CPT, and Monte Carlo simulations become drastically simplified.

Fig. 21(b) shows the cohf of the longitudinal effective turbulence at  $n=n_1$ ; it is worth noting that this quantity is greater than 0.9 for distances  $|s_2 - s'_2|$  in the order of 300 m. Thus, analyses and simulations can be carried out with space steps much wider than those normally used, e.g.,  $\Delta s_2 = 60 - 180$  m, without any relevant overestimation of the buffeting response.

To verify these remarks, several analyses were carried out based on different space steps and

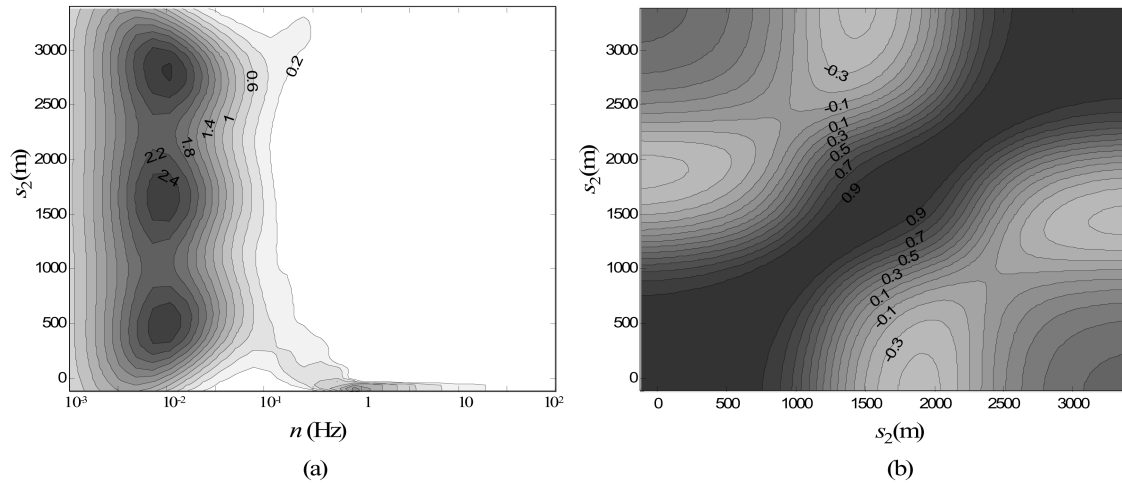


Fig. 21 Spectral (a) and coherence (b) properties of the effective turbulence field

approximating the turbulence eigenvectors with constant values, confirming that a looser spatial discretisation and turbulence modes evaluated at a constant frequency within the harmonic content of the effective turbulence lead to precise solutions. Similar results were obtained by Monte Carlo time domain simulations characterised by increasingly wider time steps and frequency independent POD modes.

The possibility of strongly reducing the computational burden of Monte Carlo simulations and finite elements analyses allows the collection of wide ensembles to produce accurate statistical estimations. The extrapolation of these considerations to nonlinear dynamic analyses of the response requires some cautions but seems very attractive especially for complex and burdensome problems as the Messina Straits Bridge project.

#### 4. Conclusions and prospects

POD was developed over the last century in many different fields, originating a broad band of fragmentary and variegated methods and applications, whose collation requires working out a comprehensive viewpoint.

This paper provides such a comprehensive viewpoint, showing that a sound and robust position of the problem involves all the tools to deal with random vectors, finite-energy random processes, infinite-energy random processes (above all stationary processes) and incompletely-stationary random processes in a unique and homogeneous environment. Linear transformations of multi-variate random processes and Monte Carlo digital simulations can be dealt with as particular cases and applications belonging to such an environment.

The search for the covariance and spectral modes of multi-variate stationary processes, which covered almost all the applications in wind engineering (Solari, *et al.* 2007), represents a special topic in the field of linear transformations which, in their turn, can be interpreted as a basic but limited ingredient in the broad class of POD tools.

Some of these tools are examined with reference to four applications developed at the University of Genoa, suitably revised and embedded into the proposed homogeneous framework. Within the

class of stationary random processes, the problems related to the modelling and simulation of turbulent fields, the representation of the aerodynamic forces on a tall building model and the buffeting response of a long-span bridge are analysed. An application of POD for the digital simulation of the nonstationary turbulence field experienced by an aircraft moving along a trajectory is also proposed.

The use of those tools still little applied in wind engineering, for instance the analysis of non-stationary and/or not homogeneous processes, typical of aeolic phenomena with small temporal and/or spatial scales, offers particularly attractive prospects of development.

## References

- Burlando, M., Carassale, L., Borghesi, M. V., Tubino, F., Ratto, C. F. and Solari, G. (2005), "Numerical simulation of turbulent wind fields at airports in complex terrain", *C.D. Proc., 4th European-African Conference on Wind Engineering*, Prague.
- Carassale, L. (2005), "Filter-based representation of the random loads on structures", *Prob. Eng. Mech.*, **20**, 373-388.
- Carassale, L., Hibi, K., Pagnini, L. C., Solari, G. and Tamura, Y. (2004), "POD analysis of the dynamic wind pressure on a tall building", *Proc., 5th Int. Coll. on Bluff Body Aerodynamics & Applications, BBAA V*, Ottawa, Canada.
- Carassale, L., Piccardo, G. and Solari, G. (2001), "Double modal transformation and wind engineering applications", *J. Eng. Mech.*, ASCE, **127**(5), 432-439.
- Carassale, L. and Solari, G. (2002), "Wind modes for structural dynamics: a continuous approach", *Prob. Eng. Mech.*, **17**, 157-166.
- Carassale, L. and Solari, G. (2005), "Monte Carlo simulation of wind velocity fields on complex structures", *J. Wind Eng. Ind. Aerodyn.*, **94**, 323-339.
- Kanwal, R. P. (1983), *Generalized Functions: Theory and Applications*. Academic Press, London.
- Kikuchi, H., Tamura, Y., Ueda, H. and Hibi, K. (1997), "Dynamic wind pressure acting on a tall building model - Proper orthogonal decomposition", *J. Wind Eng. Ind. Aerodyn.*, **69-71**, 631-646.
- Lumley, J. L. (1970), *Stochastic Tools in Turbulence*, Academic Press, New York.
- Mercer, T. (1909), "Functions of positive and negative type and their connection with the theory of integral equations", *Trans. London Phil. Soc. (A)*, **209**, 415-446.
- Papoulis, A. (1965), *Probability, Random Variables, and Stochastic Processes*, McGraw-Hill, New York.
- Phoon, K. K., Huang, S. P. and Quek, S. T. (2002a), "Implementation of Karhunen-Loeve expansion for simulation using a wavelet-Galerkin scheme", *Prob. Eng. Mech.*, **17**, 293-303.
- Phoon, K. K., Huang, S. P. and Quek, S. T. (2002b), "Simulation of second-order processes using Karhunen-Loeve expansion", *Comput. Struct.*, **80**, 1049-1060.
- Priestley, M. B. (1981), *Spectral Analysis and Time Series*, Academic Press Limited, London.
- Ratto, C. F., R. Festa, C. Romeo, O. A. Frumento, and Galluzzi, M. (1994), "Mass-consistent models for wind fields over complex terrain: The state of the art", *Environ. Soft.*, **9**, 247-268.
- Solari, G. and Carassale, L. (2000), "Modal transformation tools in structural dynamics and wind engineering", *Wind and Struct.*, **3**(4), 221-241.
- Solari, G., Carassale, L. and Tubino, F. (2007), "Proper orthogonal decomposition in wind engineering. Part 1: A state-of-the-art and some prospects", *Wind and Struct.*, **10**(2), 153-176.
- Solari, G. and Tubino, F. (2002), "A new turbulence model based on principal components", *Prob. Eng. Mech.*, **17**, 327-335.
- Tubino, F. and Solari, G. (2005), "Double POD for representing and simulating turbulence fields", *J. Eng. Mech.*, ASCE, **131**, 1302-1312.
- Tubino, F. and Solari, G. (2007), "Double modal transformation and effective turbulence for the gust buffeting of long span bridges", *Eng. Struct.*, in press.
- Van Trees, H. I. (1968), *Detection, Estimation and Modulation theory. Part 1*, John Wiley and Sons, New York.

## Notation

$A$	frequency-domain representation of $\alpha$ (Section 3.1);
$\mathbf{A}$	matrix defining aerodynamic forces (Section 3.4);
$a, b$	extremes of the interval of definition of $v$ ;
$\mathbb{C}$	set of complex numbers;
$C_v, \mathbf{C}_v, \mathbf{C}_{\tilde{v}}, \mathbf{C}_x$	covariance function or covariance matrix of the processes $v, \mathbf{v}, \tilde{v}$ and $\mathbf{x}$ ;
$\hat{\mathbf{C}}_v$	matrix of the correlation coefficients of $\mathbf{v}$ (Section 3.3);
$\tilde{C}_v, \tilde{\mathbf{C}}_v$	single-variable covariance function of the stationary processes $v$ and $\mathbf{v}$ ;
$Coh_{ij}$	coherence function of the turbulence components $v_i$ and $v_j$ (Section 3.1);
$D_{jk}, \mathbf{D}$	cross-modal participation coefficients and matrix (Section 3.4);
$\mathcal{D}$	definition domain of random processes;
$E$	statistical average operator;
$\mathbf{f}$	vector of the external forces;
$H$	unit-step function;
$H_j$	complex frequency response function of the $j$ -th structural mode;
$\mathbf{I}$	identity matrix;
$J, J_1$	functionals to be minimised in the representation problem;
$\mathbf{M}$	mass matrix;
$M$	number of degrees of freedom;
$m$	dimension of the argument of a random process;
$m$ -D	$m$ -dimensional, referred to a random process;
$n$	dimension of a vector to be represented by POD;
$n_j$	natural frequency of the $j$ -th vibration mode;
$n_s$	number of spectral modes to retain (Section 3.4);
$n$ -V	$n$ -variate, referred to a random variable or process;
$p_j, \mathbf{p}$	structural principal coordinates, vector of the principal coordinates;
$P_j$	frequency-domain representation of $p_j$ ;
$q_j, \mathbf{q}$	structural Lagrangian coordinates, vector of the Lagrangian coordinates;
$r$	abscissa along the domain $\mathcal{D}$ in the example of Section 3.1;
$\mathbf{R}_c, \mathbf{R}_s$	matrixes defining normalised forces (Section 3.3);
$\mathbb{R}$	set of real numbers;
$s, s_k$	space coordinate, Laplace variable, Fourier coefficients of the covariance function;
$\mathbf{s}$	vector of the space coordinates;
$\check{\mathbf{s}}$	trajectory in the space;
$S_v, \mathbf{S}_v, \mathbf{S}_p, \mathbf{S}_q, \mathbf{S}_y$	power spectral density function/matrix of the processes $v, \mathbf{v}, \mathbf{p}, \mathbf{q}$ and $\mathbf{y}$ ;
$S_{ij}$	cross-power spectral density function of the turbulence components $v_i$ and $v_j$ (Section 3.1);
$\hat{\mathbf{S}}_v$	coherence matrix of $\mathbf{v}$ (Section 3.3);
$t, t_k$	argument of a random process or time instants;
$T$	period of a statistically periodic process;
$u, \mathbf{u}$	scalar-valued and vector-valued test functions;
$\hat{u}, \hat{\mathbf{u}}$	Fourier transform of $u$ and $\mathbf{u}$ ;
$v, \mathbf{v}$	random process or random vector;

$\mathbf{V}$	frequency-domain representation of the process $\mathbf{v}$ ;
$\tilde{\mathbf{v}}$	turbulence field along the trajectory $\mathfrak{S}$ ;
$x_k, \mathbf{x}$	POD/covariance principal components, vector of the POD/covariance principal components;
$y_k, \mathbf{y}$	spectral principal components, vector of the spectral principal components;
$Y_k, \mathbf{Y}$	frequency-domain representation of $y_k$ and $\mathbf{y}$ ;
$z_h$	spectral principal component of $\alpha$ ;
$Z_h$	frequency-domain representation of $z_h$ ;
$\alpha$	generic turbulence component (Section 3.1);
$\delta$	Kronecker delta or Dirac function;
$\Delta t, \Delta \omega$	discrete time step and circular frequency step;
$\varphi$	vertical angle of the wind velocity (Section 3.2);
$\phi_k, \Phi_k$	POD eigenvectors and eigenfunctions, covariance eigenvectors;
$\hat{\phi}_k, \hat{\Phi}_k$	generalised Fourier transform of $\phi_k$ and $\Phi_k$ ;
$\Phi$	matrix of the covariance eigenvectors;
$\gamma_k, \Gamma$	spectral eigenvalues, matrix of the spectral eigenvalues;
$\hat{\gamma}_k$	eigenvalues of the coherence matrix (Section 3.3);
$\lambda_k, \Lambda$	POD/covariance eigenvalues, matrix of the covariance eigenvalues;
$\hat{\lambda}_k$	eigenvalues of the correlation coefficients' matrix (Section 3.3);
$\theta$	horizontal angle of the wind velocity (Section 3.2);
$\theta_k, \Theta$	spectral eigenvectors, matrix of the spectral eigenvectors;
$\vartheta_h$	spectral eigenfunction of $\alpha$ (Section 3.1);
$\sigma_i$	standard deviation of the turbulence component $v_i$ (Section 3.3);
$\tau$	$t$ -lag for the computation of covariance;
$\omega$	circular frequency or wave number;
$\omega_j$	natural circular frequency of the $j$ -th vibration mode;
$\xi_j, \xi_{jk}, \xi_{jkh}$	random numbers;
$\Psi_j, \Psi$	structural eigenvectors, matrix of the structural eigenvectors;
$\zeta_j$	modal damping ratio.